Photovoltaic expansion-limit through a net energy metering scheme for selected Malaysian public hospitals.
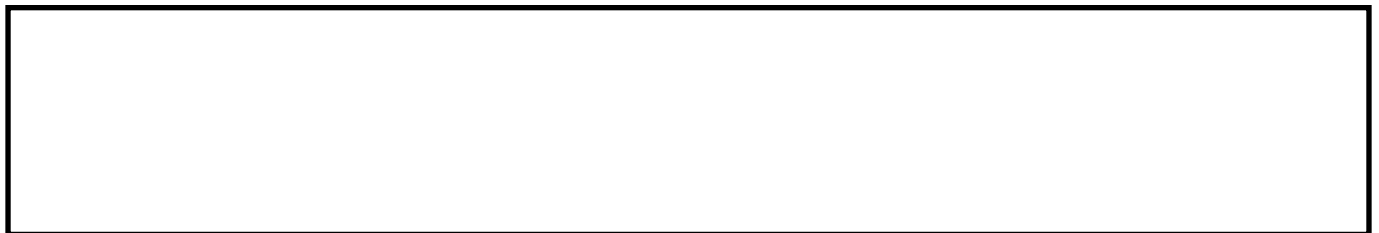
AMRAN, M.E., MUHTAZARUDDIN, M.N., MUHAMMAD-SUKKI, F., BANI, N.A., AHMAD ZAIDI, T.Z., KAMALUDDIN, K.A., ARDILA-REY, J.A.

2019

Photovoltaic Expansion-Limit through a Net Energy Metering Scheme for Selected Malaysian Public Hospitals

Mohd Effendi Amran [1,2,*], Mohd Nabil Muhtazaruddin [2,*], Firdaus Muhammad-Sukki [3,*], Nurul Aini Bani [2], Tauran Zaidi Ahmad Zaidi [1], Khairul Azmy Kamaluddin [1] and Jorge Alfredo Ardila-Rey [4]

[1]   Engineering Services Division, Ministry of Health Malaysia, Putrajaya 62590, Malaysia; tauranzaidi@moh.gov.my (T.Z.A.Z.); khairulazmy@moh.gov.my (K.A.K.)

[2]   Razak Faculty of Technology and Informatics, Universiti Teknologi Malaysia, Kuala Lumpur 54100, Malaysia; nurulaini.kl@utm.my

[3]   School of Engineering, Robert Gordon University, Garthdee Road, Aberdeen, Scotland AB10 7GJ, UK

[4]   Department of Electrical Engineering, Universidad Técnica Federico Santa María, Santiago de Chile 8940000, Chile; jorge.ardila@usm.cl

*   Correspondence: meffendi.amran@gmail.com (M.E.A.); mohdnabil.kl@utm.my (M.N.M.); f.b.muhammad-sukki@rgu.ac.uk (F.M.-S.)

check for updates

Abstract: This paper presents an optimization approach in determining the expansion-limit of Renewable Distributed Generation (DG) capacity through a Net Energy Metering (NEM) scheme specifically for selected Malaysian public hospitals. In this study, the total line loss reduction was analyzed and set as the main objective function in the optimization process where an acceptance region for DG extensiveness was proposed via the lower total line loss outcome value. Solar photovoltaic (PV)-type DG unit (PV-DG) was identified as the type of DG used in this paper. Artificial Bee Colony (ABC) algorithm was chosen to alleviate such PV-DG optimization. The distribution network uses a bus and line data setup from the three selected Malaysian public hospitals prior to three different levels, i.e., National, State, and District level hospitals. MATLAB simulation result showed the PV-DG expansion capacity towards bigger scale and location bounded by the U-trajectory shape theory which resulted in a contradiction between NEM current maximum capacity requirement and actual PV-DG expansion-limit. These limitations were also found to be different among three different level hospitals, and the expansion-limit was tailored by their own distribution network parameters. Thus, this paper provides technical justification and gives the best option to the renewable energy (RE) developer for more effective PV-DG integration through the utilization of a NEM scheme. The importance of the study is portrayed in-depth towards achieving a more sensible and accurate way of estimating the outcome. This will encourage developers, building owners, and users in participating towards achieving potential benefits both in monetary and power system reliability improvement, specifically for Malaysian public hospital applications.

Keywords: net energy metering (NEM); renewable energy (RE); artificial bee colony (ABC); distributed generation (DG); photovoltaic-type DG (PV-DG); maximum demand (MD)

---

1. Introduction

Malaysian public hospitals are organized into National, State, and District levels, where in [1] the authors differentiated these three levels as follows: **National level hospitals**—provide a comprehensive range of tertiary care services (for instance, Hospital Kuala Lumpur, which serves as the National

Referral Centre). **State level hospitals**—with one located in the capital of all 13 states in the country which provide a comprehensive range of secondary services. Finally, **district level hospitals**—provide basic inpatient care services, and those with resident specialists also provide some specialty services.

Physically, these three level hospitals are differentiated by specific range numbers of beds as well as indication outlook to determine the size, capacity, and functionality of the hospital buildings in which they are approximately uniform in each of said levels in terms of building design, operational flow, installed-equipment, energy trend, and maximum demand of energy utilization [2]. Hospitals also outfitted with various sorts of high-end microprocessor-based medical equipment such as X-Ray Machines, Computed Tomography (CT) Scans, Magnetic Resonance Imagings (MRI) machines, Angiographies, Linear Accelerator (LINAC), Mammography, Anesthetic equipment, life support machines, and so forth, which are very high load in terms of electrical power consumption; which also highlight the various types of electrical load that ought to be taken care of.

The new trend is to design and build or even operate existing hospitals guided with environmental technology in sustainability, renewable based resources, and systems design towards reducing consumption of energy as well as reducing carbon emissions in making them possible in achieving higher building performance [3]. Moreover, based on data from Ministry of Health Malaysia, 28 hospitals are identified as consuming more than 3,000,000 kWh of electricity over a consecutive period of not more than 6 months, where, according to figures by the utility provider (Tenaga National Berhad (TNB)), these 28 hospitals alone accounted for approximately 13% of the government's 2009 energy bill [3]. Similarly, with one of the neighboring countries, hospitals in Singapore, according to [4], contribute as the second highest energy consumers on a per square foot basis after the food service industry. The scenarios of two countries make the hospital building sector a significant contributor to the high-energy use, as such, the reliable determination of load characteristics becoming an important engineering task since the consumers are responsible for the assessment and maintenance of power system equipment available on their premises. [5,6]. Additionally, a sustainable approach is winding up to be more attractive in a growing number of hospitals [7]. In addition, sustainability is formally embraced in Malaysia Eleventh Plan where green growth will be a fundamental shift, especially in the human capital, policy, and regulatory framework, green technology investment, and financial instruments [8].

On the other hand, the green and efficient energy sector in Malaysia has set a 2% share of renewable energy (RE) installed-capacity in the previous year while targeted for 5.5% by the year 2015, and finally striving towards 11% of standing quota to be achieved by 2020 [9]. In line with that, the Feed-in Tariff (FiT) implementation which commenced on 1st December 2011 has foreseen the uprising RE quota towards 17% by 2020 [10,11]. However, the most recent, the 2019 initiative by Ministry of Energy, Science, Technology, Environment and Climate Change Malaysia (MESTECC) has launched a commitment to enlarge the green and efficient energy sector by increasing the percentage of RE from 2% towards 20% for electricity generation by 2025 [12,13]. Thus, the evolution of RE-based distributed generation (DG) for higher installed-capacity is expected to grow, ensuring the government key achievement can be achieved. The only scheme that allows higher capacity for photovoltaic (PV) building integration in Malaysia is Net Energy Metering (NEM) which applies to all domestic, commercial, and industrial sectors with maximum capacity up to 75% from maximum demand (MD) [13]. In this sense, the above-mentioned 20% target achievement for RE utilization as declared in MESTECC initiatives of 2019, is also involved with implementation of enhancing NEM and solar leasing which enables greater access to RE sources [12].

Based on the essence of sustainable developments, the PV-type DG (PV-DG) application is one of the most influentially common principles [14] and a consequential approach in reducing the energy consumption in buildings [15]. However, DG can worsen the system performance [16] and lead to power losses and contribute to the inefficiency of RE transmitting if the proper assessment is not well considered [3]. The reason behind the issue is that the connection of DG to radial distribution networks can change power flows from unidirectional to bidirectional affecting load-related losses [17].

Development of the distribution network is traditionally centralized and passive with radial topology, where power flow in a traditional distribution network was unidirectional and determined by the load profile [18]. With the presence of DG, the power system is changing, i.e., a large number of DG units are commonly connected to a distribution network which transform into active modern distribution network with bidirectional power flows defined by the load profile and power generation of the DG units [19]. By connecting the DG units to a distribution network, the power losses and node voltages are changing [20]. The energy loss variation as a function of the penetration level of DG according to [17,21] forms a U-shape trajectory in all the situations, which is also supported by studies in [3,22].

In further situation, when larger PV-DG scale is utilized beyond optimal value (i.e., towards 75% of MD), the actual consumption for total line losses reduction is potentially affected, and this is bound to the U-shape trajectory behavior in DG application. Thus, adoption of NEM specification of PV-DG maximum installed capacity (i.e., 75% from MD) for Malaysian public hospitals has highlighted a question, whether the scheme can be utilized with the fully maximum requirement (i.e., 75% from MD) or limited to a certain imposed maximum level, subjected to the total line losses reduction based on simulation results.

This paper proposes a PV-DG simultaneous optimization approach (i.e., both capacity and location) to identify the expansion-limit as well as the actual effective region in utilizing the NEM scheme for capacity requirement, subject to total line loss reduction. This paper also aimed for actual application in a distribution network from selected three levels of Malaysian public hospitals i.e., National, State, and District level hospital. As a further approach, 14 sequences of PV-DG capacity represented by percentage value from MD are newly formed, where the optimization simulation process is conducted to determine the total line loss reduction outcome. In contrast, segregation of 14 case ranking is made in 5% ascending order towards the maximum of 75% from MD as required in NEM, and then this simulated outcome is analyzed through a graphical U-shape trajectory plotted theory for more comprehensive understanding of the actual extension level of NEM acceptance.

The rest of this paper is organized as follows: Section 2 introduces relevant standards for PV-DG. Section 3 describes brief explanations on the adoption of the NEM scheme for PV-DG integration. Section 4 focuses on issues related to PV-DG integration and expansion through a NEM scheme. Section 5 identifies issues in PV-DG via NEM application within Malaysian public hospitals. Section 6 touches on optimization using ABC. Section 7 describes the optimization method and the problem formulation of the proposed method. Section 8 presents simulation results and discussions. Section 9 concludes the paper. The proposed assessment for PV-DG expansion purposely and specifically for Malaysian public hospitals offer a new contribution towards a unique solution for effective outcomes since these hospitals are different from other buildings in many aspects which requires a tailored solution by its own parameter setting. This also justifies the importance of the study which is portrayed in-depth towards achieving a more sensible and accurate way of estimating the outcome which will encourage the developers, building owners, and users, in participating towards achieving potential benefits both in monetary and power system reliability improvement for Malaysian public hospital application. The other contributions of this paper can be summarized as follows:

- Highlighted the discrepancies in effectiveness between NEM requirement for maximum PV-DG capacity (i.e., 75% from MD) and the simulated PV-DG expansion-limit using an actual distribution network from three selected public hospitals.
- Highlighted the U-shape trajectory loss curve theory which bounded the simulation outcome for confirming the PV-DG expansion-limit as well as the optimal value.
- Established two conditions in measuring the NEM scheme compatibleness for selected Malaysian public hospitals, i.e., whether [*expansion-limit ≤ 75% MD*] or [*expansion-limit ≥ 75% MD*].
- In contrast, this research revealed confirmation of the incompatibility of the maximum PV-DG capacity requirement in the NEM scheme for selected Malaysian public hospitals and introduced the actual figure for maximum PV-DG capacity for these three-level hospitals.

2. Related Standards for PV-DG Integration

There are various standards related to PV-DG interconnections which may influence the development of a DG system, where Wu et al. [23] had highlighted the IEEE1547 and the IEC61727 as the most widely recognized and used standards, among all related international standards. The integration of DG (below 10 MVA) is subjected to the IEEE 1547 standard which includes technical specifications and tests guidelines, while IEC61727 applies to PV power systems for utility-integration with a rated capacity of below 10 kVA through a low-voltage (LV) utility network, which also concerns the compatibility between PV systems and public networks. The IEEE 929 on the other hand, was tailored to PV systems of below 10 kW which provides practical guidelines for the operation via connection to a power system, covering personnel safety, the protection of equipment, power quality, and the operation of the utility system. Wu et al. [23] also summarized common international standards such as the IEEE and IEC standards, the state guidelines of California and Texas in the U.S, the national guidelines of Canada, UK, Germany, Spain, Australia, China, Taiwan, South Korea, and Japan, which also includes additional materials on synchronization, grounding, flickers, prevention of electromagnetic interference (EMI), isolation and switching, and short-circuit protection.

Many countries, including the US, have adopted and incorporated these international regulations into their national standards. In the Malaysia context, the Malaysian Standard (MS) for the installation and protection of solar PV system has been developed where all the requirements and currently available standards are as shown in Table 1 [24].

Table 1. Malaysian Standard (MS) related to solar photovoltaic (PV).

Standards	Title
MS 1837–2010	Installation of grid-connected photovoltaic (PV) system
MS IEC 62305 1-4:2007	Protection against lightning 　Part 1: General principles 　Part 2: Risk management 　Part 3: Physical damage to structures and life hazard 　Part 4: Electrical and electronic systems within structures
MS IEC 60364-7-712:2007	Electrical installations of building—Part 7-712: requirements for special installations or locations—solar photovoltaic (PV) power supply systems
MS IEC 61836:2010	Solar photovoltaic energy system—terms, definitions, and symbols
MS IEC 62446:12	Grid-connected photovoltaic systems—minimum requirements for system documentation, commissioning tests and inspection
MS IEC 61727:2010	Photovoltaic (PV) systems—characteristics of the utility interface
MS IEC 61730 1-2:2010	Photovoltaic (PV) module safety qualification 　Part 1: Requirements for construction 　Part 2: Requirements for testing
MS IEC 60904 1-3:2013	Photovoltaic devices 　Part 1: Measurement of photovoltaic current-voltage characteristics 　Part 2: Requirements for reference solar devices 　Part 3: Measurement principles for terrestrial photovoltaic (PV) solar devices with reference spectral irradiance data
MS IEC 61215:2006	Crystalline silicon terrestrial photovoltaic (PV) modules—design qualification and type approval
MS IEC 61646:2010	Thin-film terrestrial photovoltaic (PV) modules—design qualification and type approval
MS IEC 62109-1:2011	Safety of power converters for use in photovoltaic power systems—Part 1: General requirements

3. An Adoption of NEM Scheme for PV-DG Integration

Feed-in tariff (FiT) has been implemented in Malaysia since 2011 and reached its maximum capacity quota by the end of 2015 [25] and since the FiT becomes more mature after implementation, the government of Malaysia finally introduced the NEM scheme in early 2016 with the intention to replace the FiT by 2018 [26]. The NEM system implies that an algebraic deduction is performed between the electrical energy produced by the PV system and the energy consumption [27]. Under NEM, customers are allowed to consume the RE generated electricity under normal conditions, however, in the case of excess energy generated by the RE system, it could be sold to the TNB by feed back to the grid preferably at a certain premium or retail prices determined by the Energy Commission (EC) [25]. Energy generated that is consumed first by NEM users implies less energy will be imported from the utility grid and this translates to more savings for the consumers. These savings will be significant for consumers who fall under the high electricity tariff block. The main purpose of NEM is for self-consumption to reduce demand from the grid and hence, maximum energy demand can be mitigated during peak hours [26]. Additionally, according to Oh et al. [26], NEM was also initially allocated with a 500 MW capacity quota which needs to be evenly distributed with 100 MW per year for Peninsular and the state of Sabah (i.e., 90 MW for Peninsular and 10 MW for Sabah) over a period of 5 years (2016–2020), of which the quota is to be divided into three categories, i.e., 10% for domestic households while commercial and industrial will get an equal share of 45% each.

Additionally, Poullikkas e al. [28] reviewed the NEM application in Europe, USA, Australia, Canada, and Thailand. From the European countries view, Belgium, specifically in the Brussels region, NEM is eligible for small renewable energy sources (RES) auto-producers with a capacity up to 5 kW with two different meters, i.e., a bi-directional and a green meter are applied to measure the electricity produced by the RES auto-producer. While in the Flanders region, NEM is eligible to all RES installations up to 10 kW without direct financial compensation for the injected electricity, however the financial equivalent of the injected electricity is deducted from the overall electricity bill. In Denmark, the regulation on NEM for the electricity producers for own needs is based on the Act on electricity supply and authorizes the exception of certain producers from Public Service Obligation, which is a surcharge that every consumer is obliged to pay, and it depends on each consumer's individual level of consumption [29]. In Italy, RES systems can consume as much energy as is produced for free up to 20 kW or from 20 kW up to 200 kW, and this NEM has been commissioned since 31 December 2007. If the produced energy is higher than the actual energy consumption, the producers are entitled to RE credit (REC) for this positive balance for an unlimited period of availability and even could be used as a compensation for a possible negative balance in the following years. However, if the energy produced is less than their consumption, the difference is subjected to a payment. In the Netherlands, RES via NEM are connected to the electricity grid through a small-scale connection up to 240 A and only energy taxes have to be paid to the net electricity consumption of their systems [30]. Additionally, the RES producers also subjected to a grid use charges for injecting electricity to the grid [31,32]. In the USA, all public electric utilities are required by legislation to make available upon request NEM service to their customers. Overall 47 states apply a NEM mechanism for the promotion of RES technologies, with the exception of Alabama, Mississippi, South Dakota, and Tennessee [33]. In some Australian states, the NEM is the same concept with FiT, except that FiT requires a separate meter and pays for all local generation at a preferential rate, while net metering requires only one meter [34,35]. The FiT is also subjected to a net generation monthly payment at a higher rate than retail. Ontario of Canada allows NEM for up to 500 kW, however, RECs can only be carried for 12 consecutive months. Areas of British Columbia are allowed NEM for up to 50 kW. Systems over 50 kW are covered under the Standing Offer Program. South Central British Columbia also allows NEM for up to 50 kW. Customers are paid their existing retail rate for any net energy they produce [36,37]. New Brunswick of Canada allows NEM installations up to 100 kW. RECs from excess generated power can be carried over until March at which time any excess RECs are lost. In Thailand, RE up to 1 MW per installation which produce less than actual consumption in a monthly period is eligible for the retail tariff rate for electricity fed into

the grid [38]. Producers are also compensated at the bulk supply tariff, for net excess production with about 80% of the retail rate.

The concept of NEM-PV generating facility connection is shown in Figure 1 [39], illustrating the flow of import and export of the RE generated power to the grid and also the savings in utilizing electricity from the distribution licensee.
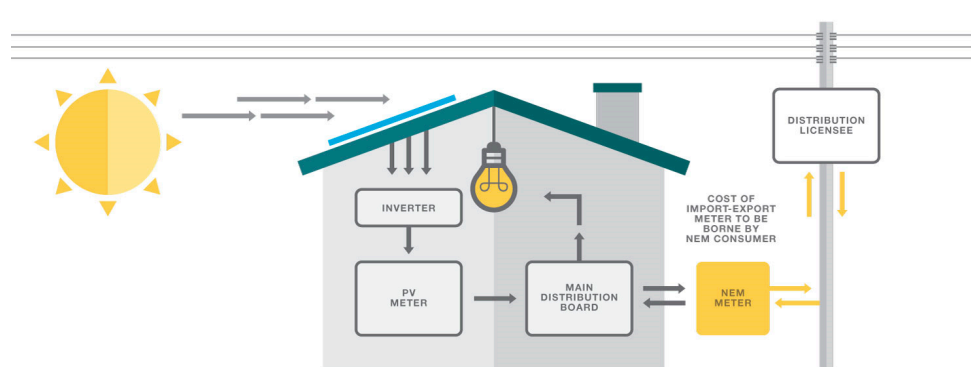

Figure 1. The concept of Net Energy Metering (NEM)-PV generating facility connection [39].

By referring to the Technical Guideline and Act related to NEM [39,40], the maximum PV installed-capacity for commercial and industrial consumers shall be 75% of maximum demand (MD) of the consumer's current installation (for current transformer metering), whichever is lower (i.e., the MD is either based on the past 1-year average of the recorded maximum demand of the consumer's installation, or the declared maximum demand for consumers for less than 1 year).

Focusing on the medium voltage (MV) electricity connection since the selected Malaysian public hospitals power system were developed, linked, and owned 11 kV system consumers, a NEM scheme can be applied via Type B for the MV consumers category, where the termination points for PV connection are located at the consumer main-switchboard (MSB) as shown in Figure 2 [40].
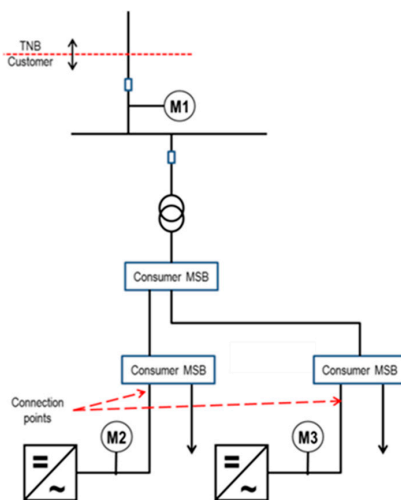

Figure 2. PV type B connection for medium voltage (MV) consumers [40].

The previously-mentioned PV integration as DG installation guided by NEM can potentially reduce the power losses and this can be determined by using Equation (1). A two buses simple test can be used to consider this situation, as shown in Figure 3 [41].

$$P_{Loss} = I_{12}^{2}.R_{Line} \quad . \tag{1}$$

The implementation of DG closer to the load site, i.e., generator G2 in Figure 3, leads to a reduction of the current I_{12} through the distribution line, and reduces the line losses. This can be proven by using Equation (1) where the reduction of I_{12} will proportionately reduce P_{Loss} of the said network. The change in the unidirectional flow of intake into more buses, i.e., the addition of generation at a load bus also will affect the real power losses and their loss sensitivities to generator outputs and the variations will occur either via sign or magnitude or both. Hence, proper placement of the DG units may reduce system losses; however, some placements can cause power losses to increase [42]. Therefore, identification of the best location and size of DG given the option of resource availability is important in order to minimize losses [43].
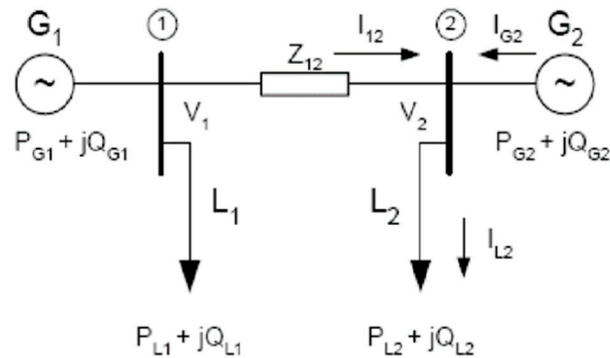

Figure 3. Bus test via distributed generation (DG) integration into network [41].

4. Issues Related to PV-DG Integration and Expansion through NEM

The injected DG in the distribution system may increase or decrease power losses level, subjected with dependability to the type of DG technology, penetration, level of dispersion, characteristics of distribution network, and load demand levels [21]. This also may even lead to greater losses compared to losses without DG [41], while, the improper size and placement of DG may increase the system losses [42,44]. A study by [45] indicated that the higher system losses caused by this improper size and placement of these DG units are due to the effect of reverse power flow from larger DG units. According to [41], loss reduction via DG is most effective when a feeder has a high load of high resistance with a low load of power factor, whereas, feeder reactance is negligible unless the DG unit operates in voltage control mode [46]. Therefore, insertion of DG in a distribution network shall consider the loss reduction element as the most important factor in its planning and operation [43].

Since distribution networks such as public hospitals, were originally designed as passive with the unidirectional flow, delivering of power is performed from the more heavily reinforced transmission system to consumers, where real and reactive power generally flow towards the downstream of the system in the direction of the voltage gradient [41]. PV-DG integration in parallel with the existing system results in an active network with operation to transport the possibility of bidirectional power flows, i.e., commercial loading condition, a change in losses, and variations in voltage [47]. In this network with PV-DG integration, line loss minimization is a matter of delicate balance between distribution losses and storage losses which need to ensure both losses are minimized [41]. In addition, these effects on the distribution level also depend on different types of loads which generally consists of residential, commercial, and industrial loads [48–50] as shown in Table 2. According to [49], the active and reactive power components respond differently to variations in the voltage and frequency of the above-mentioned three types of loads. Voltage-dependent load model is a static load model that represents the power as an exponential function of the voltage, represented as in Equations (2) and (3) [49].

$$P = P_0 V^{\alpha}, \tag{2}$$

$$Q = Q_0 V^{\beta}, \tag{3}$$

where *P* and *Q* is the real power and reactive power respectively.

Table 2. Load type and exponent value.

Load Type	α	β
Constant Impedance (CI)	2	2
Constant Current (CC)	1	1
Constant Power (CP)	0	0
Commercial (C)	1.51	3.4
Residential (R)	0.92	4.04
Industrial (I)	0.18	6

On top of dependency to the characteristics of distribution network and load demand levels, the increase or decrease of power losses level is also subjected with dependability to the type of DG technology, penetration, and level of dispersion [21], thus, types of DG used are also important to be identified. Major types of DG are categorized into four types based on power delivering capability [43,51–54], as shown in Table 3.

Table 3. Major types of DG.

DG Type	Type Description	Example
1st Type	DG is capable of injecting both real and reactive power	Synchronous generators
2nd Type	DG is capable of injecting real power but consuming reactive power	Induction generators such as wind generation farms
3rd Type	DG is capable of injecting real power only	PV, micro turbines, and fuel cells integrated to the main grid with converters/inverters
4th Type	DG is capable of injecting reactive power only	Synchronous compensators

Based on above-mentioned issues, there is a gap in determining the actual limitation for PV-DG effective criteria and also a lack in adopting the optimization baseline approach via total line losses reduction as an objective function for the initial simulating stage.

In another perspective, the presence of PV-DG may also introduce other issues such as voltage rise, thermal overload, upstream reverse power flows, frequency or voltage instability caused by cloud transient or grid faults, a reduction in system inertia and consequently reduced frequency stability [55–57]. However, the solution of the above issues can be determined according to [55,56] as follows: through consideration of the right response times; inverters, switched-capacitors, and on-load tap changers are useful devices for mitigating the voltage-rise problem. On the other hand, the thermal load problem can be solved via reconfiguration of the network by rearranging the load and PV power between phases. Active power curtailment and the determination of the PV inverter size is also important, even though the provided reactive-power support by PV inverters is considerably accepted as a means of regulating voltage, it also puts more technical stress on the inverters, so most previously established PV systems are controlled to maintain a power factor of unity. The problem of the dynamic impacts of cloud transients or grid faults can be mitigated via static compensators, energy storage systems, PV inverter control, and PV curtailment devices.

The optimization as a focus of the study depends on several factors, such as loss, voltage deviation, stability, and others, where in [55] the authors highlighted the differences of used objective functions such as the minimizations of curtailed PV energy [58], voltage deviation [59], transformer tap changer switching [60], and network losses [61,62]. Network loss is among the contributors to the optimal

problem which also is a measure in an evaluation towards the PV-DG performance. Relatively, simultaneous optimization criteria for RE-based DG location and capacity was found to be more effective to be observed via minimal losses outcome [63] and also implemented in many recent kinds of literature [63–66], however, this mechanism for estimating the possible PV-DG impact, was rarely used in current NEM application. By adopting this approach, the extensiveness of PV-DG utilization in current NEM Schemes can be improvised for a more justified and effective PV-DG measure as well as during early-stage design and estimation.

5. The Focus of Related Issues in PV-DG via NEM Application Within Malaysian Public Hospitals

An assessment for PV-DG installation purposely and specifically for Malaysian public hospitals offer a new contribution towards a unique solution for effective outcomes since these hospitals are different from other buildings in many aspects, as illustrated in Figure 4.
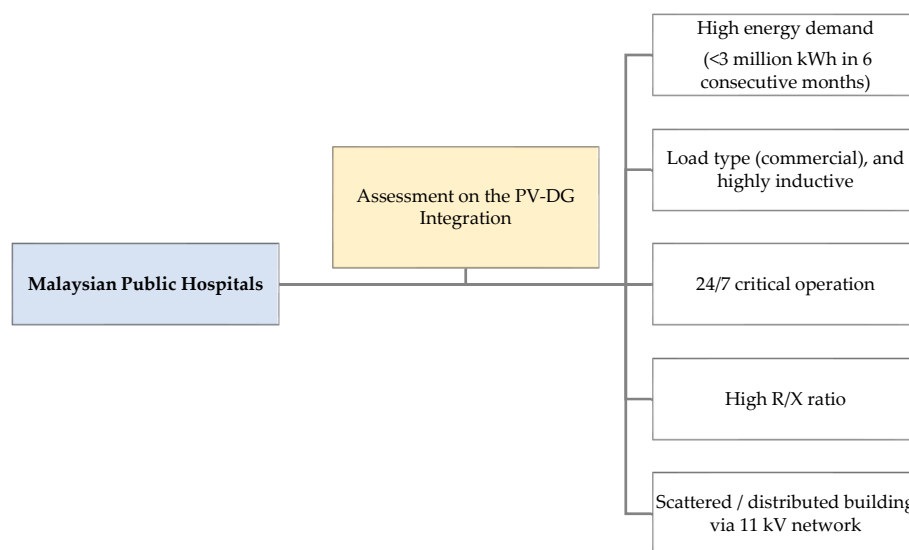
Figure 4. The significance of the PV-DG expansion-limit assessment for Malaysian public hospitals.

From Figure 4, the initial PV-DG estimation for installed capacity in Malaysian public hospitals shall be tailored by their own parameter baseline due to five main behaviors that governed their distribution network system. Malaysian public hospitals consumed high energy demand as they use energy in many different ways. Based on the 2009 government utility bill, 28 out of hundreds of public hospitals in peninsular Malaysia consumed more than 3,000,000 kWh of electricity over a consecutive period of not more than 6 months which approximately contributed 13% of the government's energy bill [3]. This range of consumption is categorized as a high energy consumer by the Regulations of EC [6]. On the other hand, due to 24/7 operation, they lead to load more air conditioning in preserving the indoor environment as well as indoor air quality and fresh air in most parts, in-spite of the tropical climate and hot humid area which need a high level of air conditioning due to level of temperature and humidity [67]. This significantly makes public hospitals constantly contribute to high electrical energy demand.

Most of the loads in a distribution network are inductive in nature [68], and additionally, since hospitals highly consume air conditioning in preserving the indoor environment as well as indoor air quality and fresh air in most of the areas as according to Moghimi el at. [67], this results in higher inductive loads due to the nature of motor or compressor-based loads [69]. Thus, loads are more inductive for Malaysian public hospitals in this sense. High inductive loads also result in the lagging Power Factor (PF) of the system which may increase network losses, voltage profile, and the system security may deteriorate [68].

In terms of building design, most of the Malaysian public hospitals are scattered in a physical building arrangement or department on a large section of land in which the electrical distribution network is radially linked to each of the said buildings via an 11 kV network. In contrast, each of the buildings is attached with their own sub-station to place the switchgear, step-down transformer, etc. For instance, a National level hospital is comprised of approximately 12 main blocks on 150 acres of land, a selected State level hospital comprises of nine main blocks on 40 acres of land, and a selected District level hospital with four main blocks on 20 acres of land. Due to this area factor, the public hospital's distributed network requires a long distance of power cables length which causes a high value of the resistance over reactance (R/X) ratio. This inherent high R/X ratio caused the voltage regulation by reactive power measure to be less effective [66]. Therefore, in such networks, active power regulation plays a more significant role in maintaining stable operation of the system. High R/X ratio in distribution networks also results in large voltage drops, low voltage stabilities, and high power losses [70]. The further consequences of PV-DG presence in this high R/X ratio affects several technical issues such as voltage rise, reverse power flow, unintentional islanding, voltage unbalance, etc. [66]. Thus, the significant issue in PV-DG integration within Malaysian public hospitals networks is the reverse power flow in which the impact will determine an extraordinary outcome of total line losses which require a tailored solution by its own parameter setting for PV-DG design.

All factors as previously mentioned affect the landscape of total line losses reduction methodology, where the effective PV-DG penetration level versus power losses presents a theory of U-shape trajectory behind obtaining the outcome [65], therefore, the non-optimal placement of PV-DG may increase the power losses resulting in a voltage profile lower than the allowable limit [17,42]. Therefore, the total line losses are chosen as the main objective criteria for the optimization process and role as the main part of this study. Thus, all the above-mentioned significances have portrayed the importance for this study towards more sensibly measuring accurate estimation outcomes and attractive encouragement among developers, building owners, and users, in participating towards achieving potential benefits both in monetary and power system reliability improvement for Malaysian public hospital applications.

6. Optimization Approach for Loss Reduction Element

As part of the objective in proposing the right parameter setting for PV-DG integration specifically in minimal power losses within voltage regulation, the analytical approach of optimization is needed. The distribution system dissipated approximately 13% of losses from power generation and these losses are categories as active power loss and reactive power loss as given by Equations (4) and (5) [71];

$$P_{Loss} = I_{ij}^2 . R_{ij} \ , \tag{4}$$

$$Q_{Loss} = I_{ij}^2 . X_{ij}, \tag{5}$$

where, I_{ij} is current flowing between i_{th} and j_{th} bus, R_{ij} and X_{ij} are resistance and reactance of branch ij respectively.

Optimization as a solution for the above problem is a procedure in identifying the value of minimum or maximum of a function by specifying several numbers of constraints known as the 'variables' [72]. Using simulation tools, the optimization function is called cost or fitness, or objective function is sequentially calculated [73]. Based on [16], separate analysis and simultaneous analysis are two identical ways of solving power losses mitigation by DG. Using separate analysis, location and capacity of DG identification are calculated separately using sensitivity factor [74] followed by an optimization technique respectively. While, in the simultaneous analysis which offer better results than separate analysis [75], this method determines the capacity and the DG location at the same time (simultaneously) by using optimization techniques, for instance, Particle Swarm Optimization (PSO), Genetic Algorithm (GA), and Artificial Bee Colony (ABC) [16,41].

Known as a population-based meta-heuristic algorithm, particle swarm optimization (PSO) works in two steps, which are calculating the particle velocity and then updating the position [50]. Using

PSO, Muttaqi et al. [76] defined capacity and location of DG which use a maximum (cost-related) performance index as the optimizing criteria and set operating current, voltage limits, and power flow balance as the constraint. The study found that reliability and investment costs have more impact on total utility expenditure than technical performance (i.e., voltage stability and line loss). DG penetration also increases in the case of high-reliability penalty (i.e., presence of critical loads). The optimal size and optimum location for renewable DG placement in the radial distribution networks by a reduction in real power losses and enhancement in voltage profile have been determined using implemented PSO technique by Kansal et al. [77] and Zareiegovar et al. [78]. This study also indicates that PSO easily suffers from partial optimization. A wide range of technical issues, i.e., active and reactive power losses of the system, the voltage profile, the line loading, and the MVA intake by the grid in renewable DG planning has been considered by El-Zonkoly [79]. PSO requires little memory and reduces the computation time, however, based on [50], studies by [77], [79], and [80] indicate that PSO easily suffers from partial optimization.

Genetic algorithm (GA) as another optimization technique, can be used to solve the non-dimensional, non-differential, and non-continuous problems which are also easy to understand. Using GA, Merei et al. [81] identified capacities of solar PV, wind turbine, and diesel generators including selection and (power and energy-related) capacity of battery system prior to minimum net present cost (NPC) as the optimization criteria. In addition, energy balance, battery state of charge limit, battery capacity limit, DG nominal power range, and minimum diesel generator operational period were set as the constraints. The findings revealed that redox-flow battery results in the most feasible design with lowest NPC. In addition, it was found that multiple battery design is not favorable for economic reasons. Yang et al. [82,83] proposed a method for a hybrid system which supplies power for a telecommunication relay station, in which the configurations of a hybrid solar-wind-battery bank system is optimized via GA. In this case, the number of PV modules, wind turbines and batteries, the PV slope angle, and wind turbine tower height were set as the decision variables. Koutroulis et al. [84] proposed an optimal size of standalone PV-wind systems using GA to select the optimal number of units with minimum cost, in line with the fulfilment to load demand. Moreover, GA based optimal sizing of desalination systems by PV-wind generators as a power supplied unit also has been presented in another study by Koutroulis and Kolokotsa [85]. Two principle aims of annualized cost minimization and minimization of the loss of power supply probability (LPSP) are satisfied via optimized sizing of a hybrid solar-wind-battery system proposed by Ould Bilal et al. [86] through multi-objective GA. There is a limitation in GA applications in real time performance due to less convergence speed and random solutions approach [87]. On the other hand, a study by Moradi and Abedini [70] observed a combination of GA and PSO algorithms for DG optimal capacity and location.

Karaboga, in 2005 [88], introduced the artificial bee colony (ABC) algorithm where this optimization algorithm initially was proposed for unconstrained problems. Then, in dealing with constrained problems in optimization, an extended version of the ABC algorithm was established [89]. Based on [90], the analogy of ABC is that three groups i.e., employed, onlookers, and scout bees, are assigned in the colony of artificial bees. An 'onlooker' is the decision maker to choose the source of food while an 'employed' is a bee going to the food source visited by the previous bee. The third one named 'scout' is a bee which carries out random searches.

Solving a placement problem of Renewable DG via ABC has been proposed by Hussain and Roy [88] and Lalitha et al. [90] where the objective function was to minimize the total system real power loss subjected to equality and inequality constraints. Comparison of results also has been made with other existing methods, such as AM and PSO to prove the validity of the proposed method, which concluded that ABC exhibited more excellent solution quality, fast convergence characteristics, and the potential for solving complex power system problems. Sohi et al. [91] implemented ABC for loss reduction and line capacity improvement in renewable DG planning problem. The mixed integer nonlinear optimization problem was solved by Abu-Mouti and El-Hawary [92] using ABC with the aim of minimizing the total system real power to determine the optimal renewable DG location,

size, and power factor. Muhtazaruddin et al. [16] proposed ABC to determine the optimal DG and capacitor coordination simultaneously on the 33-bus test system. The simulation results show that the simultaneous approach provides better power loss reduction and voltage profile enhancement compared to a separate analysis.

The review of the different metaheuristic methods proposed in the recent literature confirmed that there is no standard and generalized optimization technique capable for solving with accuracy all problems related to power system planning and control, whereas, the drawbacks of the majority of metaheuristic methods are related to the parameter adjustment and coordination between exploration and exploitation to achieve the desired near global solution [22].

7. Research Method

In this paper, the DG costing and the other associated financial worth analysis are not considered in solving the sizing and location problems. The simulation processes are performed in 14 case studies excluding one case for optimal value (location and size simultaneously) which uses selected distribution network of three selected Malaysian public hospitals, i.e., National level, State level, and District level hospitals. The distribution network also comprises of six actual power system parameters, consisting of distribution bus identification, active power load (P), reactive power load (Q), resistance (R), and reactance (X) for laid cables (Ω/km) and voltage level (V) as shown in Appendix A (Tables A1–A3) for National level, State level, and District level hospitals respectively.

The distribution network in a National level hospital is fed by three different intake supplies (i.e., from the utility provider) through its radial network, however, the bus arrangement for simulation is only divided and performs in two main zones namely Zone A and Zone B. This scenario is similar with State and District level hospitals where the division of zoning for simulation are formed into two zones (Zone A and Zone B) for the National level, and one zone (Zone A) for District level hospitals.

All simulations were performed using MATLAB programming. In previous optimal DG studies, analysis for both capacity and location of DG were conducted separately, which means power loss reduction is achieved by determining optimal output power and location of DG individually [16,93]. Thus, the solution might be trapped in a local optimum since the solution to determine optimal DG coordination is not based on optimal location, and vice versa. For the global optimum solution, both DG size and location were identified simultaneously. Photovoltaic DG type (3rd Type) was set in simulation coding as in DG identification (Table 3) where only real power output is transmitted into the network.

ABC is proposed in this paper for solving the PV-DG optimal capacity and location via MATLAB simulation. The algorithm of ABC assigned employed artificial bees in the first half of the colony, consequently, the onlookers, which constitutes the second half. It was specified that only one employed bee was assigned to every food source. Whereby, in the case of an exhausted food source the employed bee and onlooker bees becomes a scout, according to Equation (6). In the initialize stage, the bees select sets of food source positions randomly and determine their nectar amounts. Within the hive, the nectar source information is shared among the bees waiting on the dance area by the coming bees into the hive. By this initial information, the existence of food source is kept in memory, of which, all employed bees make their way to a previously visited cycle food source. Concurrently, a new source of food is also being visualized in the neighborhood of the present path via comparison-based positions of the food source. Next, the preferred food source area by an onlooker depends on the distributed nectar information by the employed bees on the dance area. The probability of which an onlooker chooses that food source increases as the nectar amount of food source increases. This can be translated into Equation (7). Once the limit is reached, these bees leave the nectar of a food source, where a new food source is randomly identified by a scout bee and superseded with the leaving one. The ABC flowchart as illustrated in Figure 5 [94]. The process is repeated until the maximum cycle that has been set by the

user is reached. The updating formula for the above-mentioned types of bees (employed, onlooker, and scout bees) is described as in Equation (8).

$$F_i = \frac{1}{(1 + Obj.Func_i)}, \tag{6}$$

where, F_i is the fitness for the objective function and *Obj.Func$_i$* (total power loss) is the target of the study.

$$prob_i = \frac{F_i}{\sum_{i=1}^{N} F_i}, \tag{7}$$

where, $prob_i$ is the probability and N is a number of employed bees.

$$x_{ij}^{new} = x_{ij}^{old} + range(0,1) \times \left(x_{ij}^{old} - x_{kj} \right), \tag{8}$$

where, x_{ij}^{new} and x_{ij}^{old} represent the new and old (previous) value of a variable (either DG location or DG size) respectively. x_{kj} is a neighbor value that is selected randomly from jth dimension and $range(0,1)$ is a random value between 0 and 1.

$$x_i^{j\ (new)} = min(x_i^j) + range(0,1) \times \left(max(x_i^j) - min(x_i^j) \right), \tag{9}$$

where, applies to all jth dimension and $range(0,1)$ is a random value between 0 and 1.
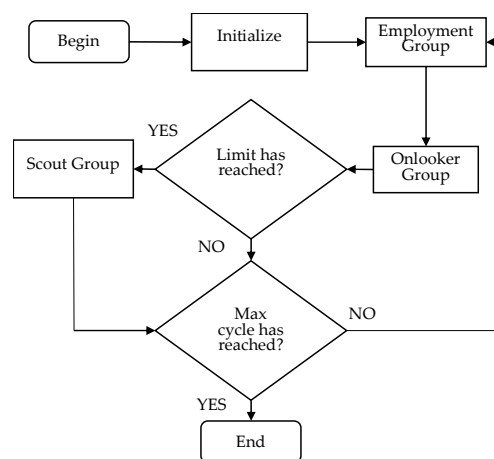

Figure 5. Flowchart of artificial bee colony (ABC) [94].

The Pseudo Code for the ABC algorithm in searching the optimal DG output to minimize power losses in the distribution system is performed using the following steps:

Step 1　Initialization of the food source positions.

Step 2　Calculate the nectar amount of the population by means of their fitness values using Equation (6)

Step 3　Produce neighbor solutions by using Equation (8) for the employed bees and next, evaluate them as in **Step 2**.

Step 4　Apply the selection process.

Step 5　If all onlooker bees are distributed, skip to **Step 9**. Otherwise, go to the next step.

Step 6　Calculate the probability values using Equation (7) for the solutions

Step 7　Produce neighbor solutions for the selected onlooker bee, depending on the value, using Equation (8) and evaluate them as indicated in **Step 2**.

Step 8　Proceed with **Step 4**.

Step 9   Identify the scout bees abandoned solution, if it exists, replace it with a completely new solution via Equation (9) and the evaluation as indicated in **Step 2**.

Step 10   Memorize the best-attained solution.

Step 11   Stop if cycle = maximum cycle number (MCN) and display the result, else, proceed **Step 3**.

The selection of algorithm type is no concern since the contribution of this study mainly focuses on assessment towards bridging the gap of effectiveness between NEM requirement for maximum PV-DG capacity (i.e., 75% from MD) and the simulated PV-DG expansion-limit. In addition, the distribution networks from selected public hospitals which were used for the simulation are less complex in terms of number of buses compared to the others that have been used in the related literature, where multiple algorithms did not cause many differences in the outcome value. This can be proven through the comparison making between the ABC's initial power loss outcome (without any integration of PV-DG) and optimal loss reduction outcome with the simulated result via PSO algorithm, where the accepted proximity range of output value from both methods shall fulfill the above expectation and significantly validates the overall coding setup process.

Despite that, a study by Abu-Mouti and El-Hawary [92] was additionally considered in choosing ABC where it was claimed to be simple, have ease for implementation, and capable of handling the complex (added value to the study) optimization problems, therefore, ABC was chosen in the MATLAB simulation. Their study also was conducted with five cases of simulation where the algorithm relatively converged in fewer maximum cycle number (MCN) and its robustness was proven. To portray the ABC advantages, Abu-Mouti and El-Hawary [92] also compared the proposed ABC algorithm results with the obtainable solutions by the Analytical Method and GA method. The result showed that ABC has better solution quality and convergence characteristics. Since the standard deviation of the results attained for 30 independent runs is virtually zero, the proposed ABC algorithm has confirmed its efficiency.

Total Line Losses (*TLL*) in this distribution network was selected as the main target, i.e., objective function, in ABC optimization. Equation (10) represents the formula for the objective:

$$TLL = \sum\nolimits_{L=1}^{n} \left(|I_L|^2 \times R_L\right), \tag{10}$$

where *L* is a number of branches, I_L is branch current, and R_L is the branch resistance.

The DG system performance decreases due to line losses, and due to variation of voltage level, the location and capacity of DG sources are found to be more important in dependability on the system losses and voltage stability measure as compared with several other objective function settings [95]. In contrast, simultaneous optimization criteria for RE-based DG location and capacity is found to be more effective to be observed via minimal loss outcomes [63] and have been implemented in many recent kinds of literature [63–66].

According to Box [96], line loss is the erosion of voltage over a long distance caused by the resistance of the feeder cables. The severity of line loss increases with the amount of current carried by a particular conductor, but generally, line loss starts to become apparent in feeder cables longer than 100 feet. Box [96] also highlighted the three major variables that affect the amount of line loss i.e., conductor length, cable thickness, and amperage load based on three principles. For the first principle, the resistance of a conductor increases directly with its length. The longer the run, the greater the line loss. In the second principle, the resistance of a conductor decreases in proportion to its cross-sectional area, in which the larger the conductor, the smaller the line loss. For the third principle, voltage drop varies directly with the load. The larger the load amperage, the larger the line loss. Since both the long distance of cables (due to scattering of buildings) and high amperage load are included in the five main behaviors of Malaysian public hospitals as in Figure 4, the total line losses are the best option and was chosen as the objective function in ABC optimization, which is also a way forward to highlight the uniqueness of the hospital's outcome parameter in PV-DG assessment.

Consequently, the effectiveness of the proposed PV-DG assessment was performed by simulation on the distribution network of three types of public hospital, i.e., National, State, and District hospital as presented in the Introduction, and the results obtained are graphically plotted for U-shape trajectory determination. The *P* load and *Q* load sample data of the distribution network represents the highest value within a period of six consecutive months considering the MD and maximum irradiation adopted from timeline used in collecting the energy trend via Efficient Management of Electrical Energy Regulation 2008, published by Energy Commission of Malaysia [6]. The main area of this paper only focuses on active power loss rather than reactive power loss, with the assumption that reactive power loss can be compensated via capacitor banks or other methods.

The overall flow of this study is as illustrated in Figure 6. All processes were examined for National level, State level, and District level hospitals. In the first process, the initial power loss was identified which represented the original losses of distribution network without the integration of PV-DG. This loss result, L_1, was recorded for further comparison. Next, based on the ABC algorithm setup, the optimal P_{DG1} for capacity and location (simultaneously) was obtained. At this stage, total line losses L_2 shall be much lower than L_1.
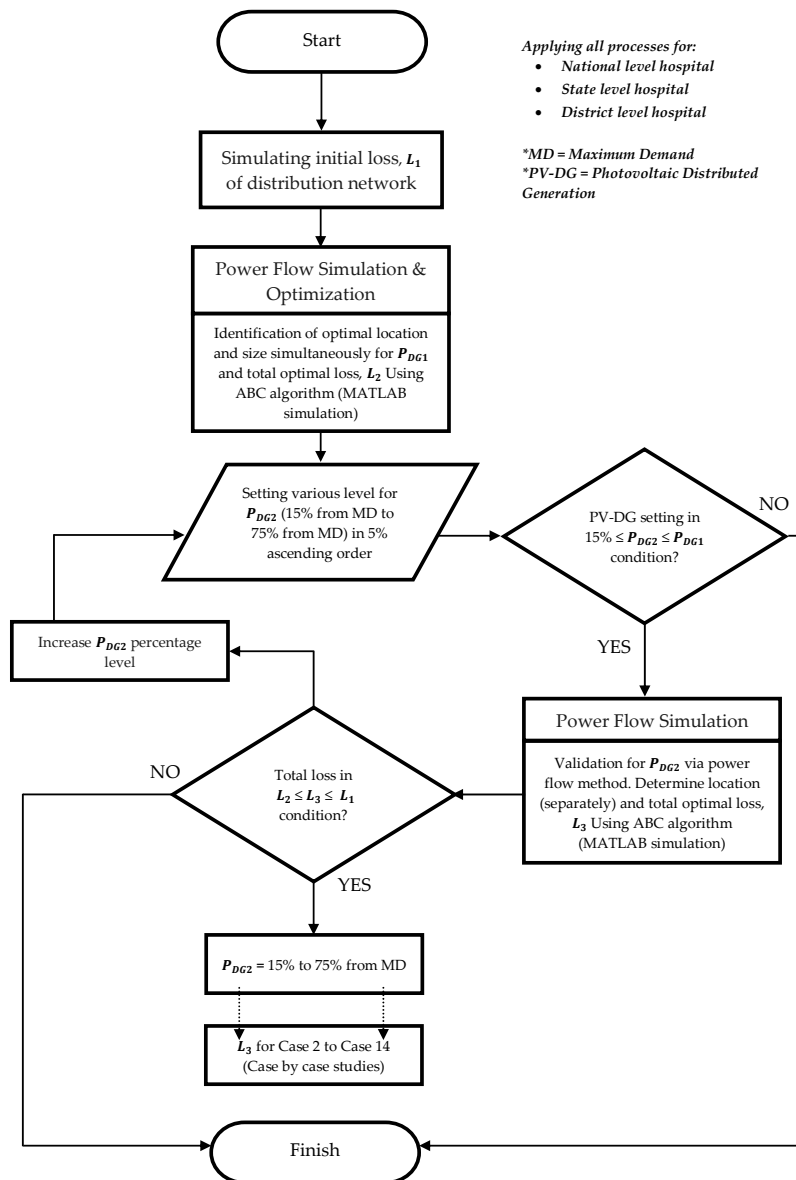

Figure 6. Overall flowchart of the study.

Optimal selection of parameters that were determined by the ABC must fulfill all constraints while striving to achieve the main objective to reduce the power losses. This important procedure needs to be observed during the optimization process to ensure violation of any limit does not occur in the solution. The optimization process with all constraints for unlimited and limited capacity is as listed below:

7.1. Size of DG Constraint

$$P_{DG(min)} \leq P_{DG1} \leq P_{DG(max)}. \tag{11}$$

$P_{DG(min)}$ and $P_{DG(max)}$ for the most optimal PV-DG value is set between 0.3 and 3 MW respectively as determined in Table 4.

$$P_{DG(min)} \leq P_{DG2} \leq P_{DG(max)}. \tag{12}$$

The minimum and maximum size of limited PV-DG ($P_{DG(min)}$ and $P_{DG(max)}$) is set between 0–15% MD to 0–75% MD in 5% MD ascending sequence as determined in Case 2 to Case 14 respectively in Table 4. The optimal value (PV-DG capacity and location) is expected to appear between these cases.

Table 4. Case by case studies performed in MATLAB simulation.

Fixed	Optimal	Description
	Case	
1		Original test system without PV-DG (initial loss/base case)
2		Determine PV-DG size (15% from MD), optimal location, and loss reduction
3		Determine PV-DG size (20% from MD), optimal location, and loss reduction
4		Determine PV-DG size (25% from MD), optimal location, and loss reduction
5		Determine PV-DG size (30% from MD), optimal location, and loss reduction
6	Determine variation of PV-DG	Determine PV-DG size (35% from MD), optimal location, and loss reduction
7	optimal location and size	Determine PV-DG size (40% from MD), optimal location, and loss reduction
8	simultaneously (between Case 1 to	Determine PV-DG size (45% from MD), optimal location, and loss reduction
9	14 based on simulation result)	Determine PV-DG size (50% from MD), optimal location, and loss reduction
10		Determine PV-DG size (55% from MD), optimal location, and loss reduction
11		Determine PV-DG size (60% from MD), optimal location, and loss reduction
12		Determine PV-DG size (65% from MD), optimal location, and loss reduction
13		Determine PV-DG size (70% from MD), optimal location, and loss reduction
14		Determine PV-DG size (75% from MD), optimal location, and loss reduction

7.2. Power Balance Constraint

$$P_{DG} + P_{substation} = P_{Load} + TLL. \tag{13}$$

The summation of the total power supply by substation and power output from the *DG* must be equal to the total size of load plus total line losses.

7.3. Voltage Bus Constraint

$$0.90 \leq V_n \leq 1.05, \tag{14}$$

where *n* is a number of buses in the distribution system.

7.4. Radial Circuit Constraint

For National, State, and District level hospitals, the distribution network in each case study shall remain in its radial circuit, i.e., maintaining the original condition of all off-point (OP) switchgear shown in Figures 7–9.

In a further process, the result L_2 from the simulated optimization (with fix capacity) is observed and if the condition of $L_2 \leq L_3 \leq L_1$ is true, the PV-DG expand capacity development is granted into

the acceptance list where the total line loss outcome value at this point is obtained and kept for further graphical plotting. The PV-DG expansion is repeated by increasing the percentage level of limitation to obtain remaining PV-DG output generated until the result of total line losses L_3 becoming higher than L_1, where at this stage, the value of PV-DG for integration with these selected distribution networks is no longer effective for power loss reduction.

All data related to the test system can be obtained in Appendix A (Tables A1–A3). Furthermore, all the DGs are assumed to function in PV mode while the loads are presumed to consume constant power.
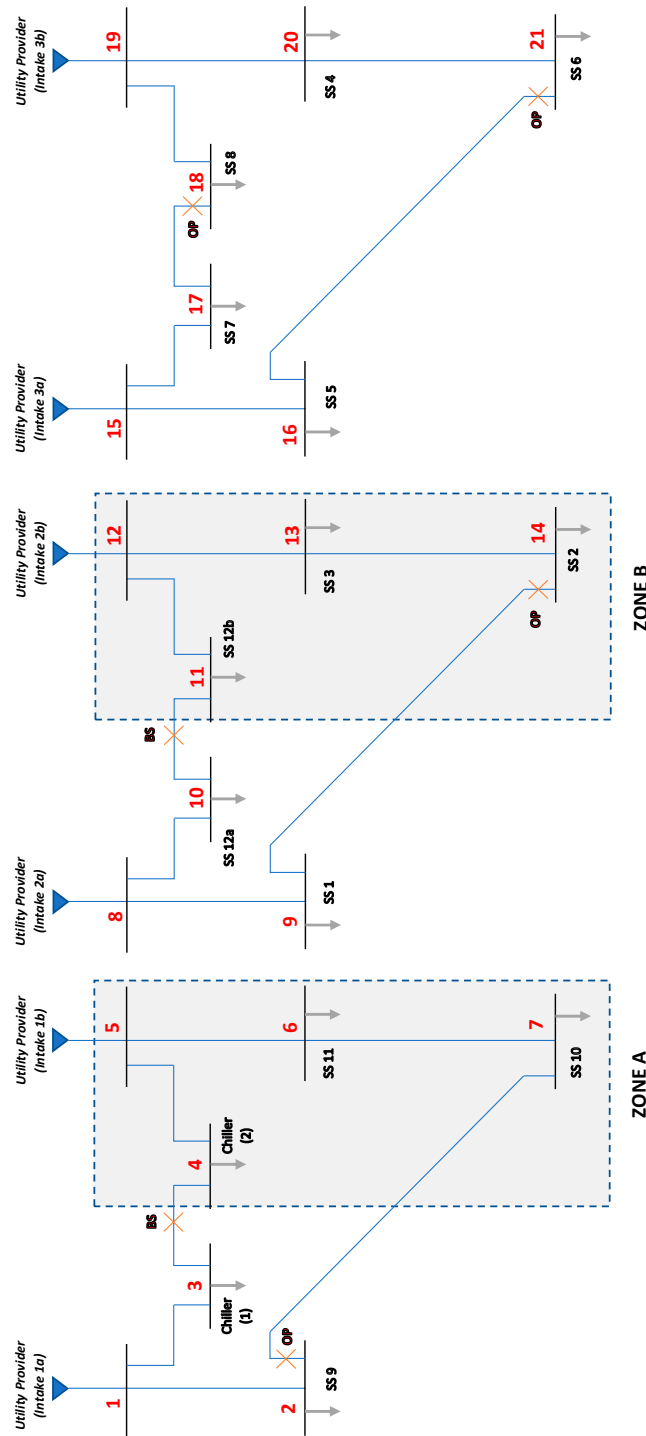

Figure 7. The distribution network of National level hospital which is simulated in two zones.
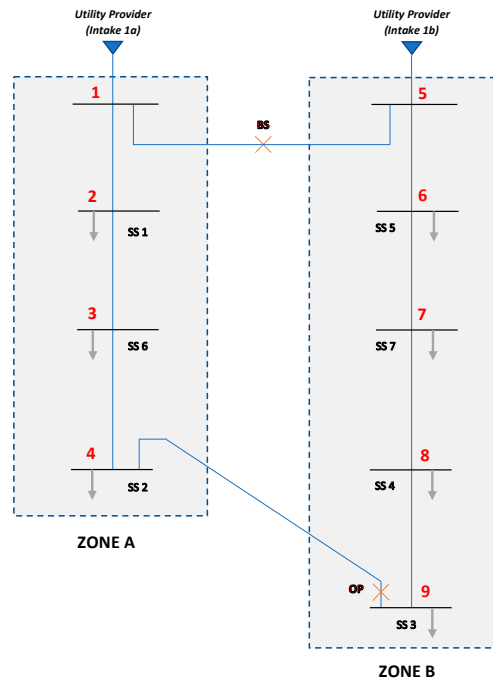
Figure 8. The distribution network of State level hospital which is simulated in two zones.
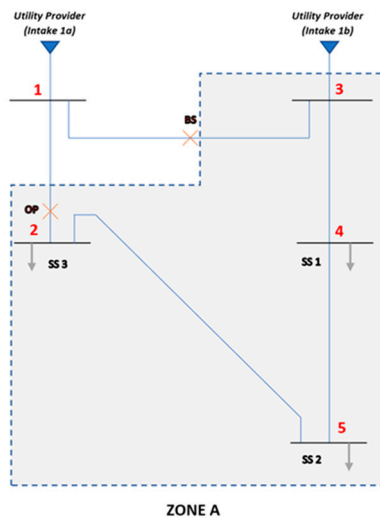

Figure 9. The distribution network of District level hospital which is simulated in one zone.

8. Results and Discussion

Tables 5–7 show the overall result for National, State, and District level hospitals respectively. These three results portray the variation of outcome figures, especially the position of the PV-DG optimal value. These results also provide conformance on the appropriateness of the current PV-DG expansion approach via NEM, either the required capacity limit can be standardized for all type of distribution networks, or the PV-DG expansion-limits are tailored by their own distribution network parameters.

8.1. Result for National Level Hospital

From the results in Table 5, simulated initial total line losses outcome via ABC (without P_{DG2} integration) as in Case 1 for Zone A and Zone B are compared with the simulated outcome value via PSO for validation of coding setup. For Case 2 to Case 8 in Zone A, integrating P_{DG2} as specified in each case, results in L_3 with percentage reductions of 4%, 16%, 39%, 57%, 71%, 81%, and 87%,

respectively. It is observed that the most optimal P_{DG2} simulated value is located between Case 8 and Case 9 with the reduction loss percentage outcome of 89% from its initial value. P_{DG2} was also compared with PSO optimal outcome and managed to achieve a similar value which confirmed the proper setup of simulation coding in MATLAB. In further PV-DG expansion, integrating P_{DG2} as in Case 9 to Case 14 however, resulted in a decreased loss reduction percentage outcome, L_3 (i.e., increased of total line losses) represented by the decreased percentage values of 75%, 74%, 72%, 68%, 63%, and 56%, respectively.

While for Zone B, integrating P_{DG2} for Case 2 to Case 9 results in L_3 with percentage reductions of 7%, 26%, 39%, 48%, 51%, 60%, 67%, and 70%, respectively. For this radial distribution size with P and Q load data, the most optimal P_{DG2} simulated value was not at the same location as in Zone A, where it is now located between Case 9 and Case 10 with the reduction loss percentage outcome of 71% from its initial value. In further PV-DG expansion, integrating P_{DG2} as in Case 10 to Case 14 however, results in decreased loss reduction percentage outcome, L_3 (i.e., increased of total line losses) represented by the decreased percentage values of 67%, 66%, 64%, 60%, and 55%, respectively.

8.2. Result for State Level Hospital

From the results in Table 6, original total line losses in the system (without P_{DG2} integration) as in Case 1 for National level hospital is similar with Case 1 of National hospital level, which represents the initial losses and being used as a base case in the comparison with further loss reduction outcome. This value was also compared with the PSO simulated outcome for validation of coding setup purposes. For Case 2 to Case 9 in Zone A, integrating P_{DG2} as specified in each case, results in L_3 with percentage reductions of 3%, 26%, 44%, 58%, 68%, 73%, 77%, and 79%, respectively. In this Zone for the distribution parameter, it is observed that the most optimal P_{DG2} simulated value is located between Case 9 and Case 10 with the reduction loss percentage outcome of 80% from its initial value. This optimal P_{DG2} was also compared with the PSO optimal outcome and managed to achieve a similar value. In further PV-DG expansion, integrating P_{DG2} as in Case 10 to Case 14 however, results in a decreased loss reduction percentage outcome, L_3 (i.e., increased of total line losses) represented by the decreased percentage values of 67%, 66%, 64%, 60%, and 55%, respectively.

While for Zone B, integrating P_{DG2} for Case 2 to Case 11 results in L_3 with percentage reductions of 9%, 31%, 44%, 53%, 62%, 69%, 71%, 74%, 79%, and 81%, respectively. For this radial distribution size with P and Q load data, the most optimal P_{DG2} simulated-value was not in the same location as in Zone A, where it is now located between Case 11 and Case 12 with the reduction loss percentage outcome of 82% from its initial value. This optimal P_{DG2} was also compared with the PSO optimal outcome and managed to achieve a similar value. In further PV-DG expansion, integrating P_{DG2} as in Case 12 to Case 14 however, results in decreased loss reduction percentage outcome, L_3 (i.e., increased of total line losses) by 75%, 74%, and 72%, respectively.

8.3. Result for District Level Hospital

From the results in Table 7, comparison of original total line losses in the system (without P_{DG2} integration) as in Case 1 between ABC and PSO results in a similar simulated output value. Subsequently for Case 2 to Case 13 in Zone A, integrating P_{DG2} as specified in each case, results in L_3 with percentage reductions of 0.5%, 1%, 21%, 38%, 52%, 63%, 70%, 75%, 79%, 85%, 89%, and 90%, respectively. It is observed that the most optimal P_{DG2} simulated value is located between Case 13 and Case 14 with the reduction loss percentage outcome of 91% from its initial value. In further PV-DG expansion, integrating P_{DG2} as in Case 14, however, results in a decreased loss reduction percentage outcome, L_3 (i.e., increased of total line losses) represented by a value of 81%.

Table 5. Table of results for National level hospital.

	Case	1	2	3	4	5	6	7	8	Optimal	9	10	11	12	13	14
ZONE A (MD = 1097 kW)	Optimal PV-DG in kWp (Bus)	-	165 (bus 5)	219 (bus 7)	274 (bus 4)	329 (bus 7)	384 (bus 4)	439 (bus 7)	494 (bus 4)	546 (bus 7)	549 (bus 7)	603 (bus 7)	658 (bus 7)	713 (bus 7)	768 (bus 7)	823 (bus 7)
Total Line Losses (kW)	ABC	464	446	389	285	201	136	89	62	53	117	121	131	149	174	206
	PSO	465	-	-	-	-	-	-	-	53	-	-	-	-	-	-
Voltage (P.U)	V min		0.9992	0.9992	0.9999	0.9992	0.9992	0.9992	0.9992	0.9999	-	-	-	-	-	-
	V max		1	1	1	1	1	1	1	1	-	-	-	-	-	-
∑ kW Losses			0.00000	0.00000	0.00000	0.00000	0.00000	0.00000	0.00000	0.00000	-	-	-	-	-	-
Total loss reduction (%)		-	4%	16%	39%	57%	71%	81%	87%	89%	75%	74%	72%	68%	63%	56%
	Case	1	2	3	4	5	6	7	8	9	Optimal	10	11	12	13	14
ZONE B (MD = 1590 kW)	Optimal PV-DG in kWp (Bus)	-	239 (bus 14)	318 (bus 14)	398 (bus 14)	477 (bus 14)	557 (bus 14)	636 (bus 13)	716 (bus 13)	795 (bus 13)	840 (bus 13)	875 (bus 13)	954 (bus 13)	1034 (bus 13)	1113 (bus 13)	1193 (bus 13)
Total Power Losses (kW)	ABC	577	536	429	351	302	282	232	193	173	169	189	195	209	229	257
	PSO	577	-	-	-	-	-	-	-	-	170	-	-	-	-	-
Voltage (P.U)	V min		0.9995	0.9995	0.9995	0.9992	0.9995	0.9995	0.9995	0.9995	0.9995	-	-	-	-	-
	V max		1	1	1	1	1	1	1	1	1	-	-	-	-	-
∑ kW Losses			0.00000	0.00000	0.00000	0.00000	0.00000	0.00000	0.00000	0.00000	0.00000	-	-	-	-	-
Total loss reduction (%)		-	7%	26%	39%	48%	51%	60%	67%	70%	71%	67%	66%	64%	60%	55%

National Level Hospital.

Table 6. Table of results for State level hospital.

Case		1	2	3	4	5	6	7	8	9	Optimal	10	11	12	13	14
ZONE A (MD = 1248 kW)	Optimal PV-DG in kWp (Bus)	-	187 (bus 4)	250 (bus 4)	312 (bus 4)	374 (bus 4)	437 (bus 4)	499 (bus 4)	562 (bus 4)	624 (bus 3)	654 (bus 3)	686 (bus 3)	749 (bus 3)	811 (bus 3)	874 (bus 3)	936 (bus 3)
Total Power Losses (kW)	ABC	350	338	258	195	146	113	95	82	72	70	115	119	127	141	158
	PSO	350	-	-	-	-	-	-	-	-	70	-	-	-	-	-
Voltage (P.U)	V min		0.9999	0.9992	0.9999	0.9992	0.9992	0.9992	0.9992	0.9999	0.9999	-	-	-	-	-
	V max		1	1	1	1	1	1	1	1	1	-	-	-	-	-
∑ kW Losses			0.00000	0.00000	0.00000	0.00000	0.00000	0.00000	0.00000	0.00000	0.00000	-	-	-	-	-
Percentage reduction (%)		-	3%	26%	44%	58%	68%	73%	77%	79%	80%	67%	66%	64%	60%	55%
Case		1	2	3	4	5	6	7	8	9	10	11	Optimal	12	13	14
ZONE B (2584 kW)	Optimal PV-DG in kWp (Bus)	-	388 (bus 9)	517 (bus 9)	646 (bus 9)	775 (bus 9)	904 (bus 8)	1034 (bus 8)	1163 (bus 8)	1292 (bus 7)	1421 (bus 7)	1550 (bus 7)	1600 (bus 7)	1680 (bus 7)	1809 (bus 7)	1938 (bus 7)
Total Power Losses (kW)	ABC	1466	1327	1014	820	690	560	450	431	381	308	274	270	370	385	415
	PSO	1466	-	-	-	-	-	-	-	-	-	-	271	-	-	-
Voltage (P.U)	V min		0.9997	0.9995	0.9995	0.9992	0.9995	0.9995	0.9995	0.9995	0.9995	0.9995	0.9997	-	-	-
	V max		1	1	1	1	1	1	1	1	1	1	1	-	-	-
∑ kW Losses			0.00000	0.00000	0.00000	0.00000	0.00000	0.00000	0.00000	0.00000	0.00000	0.00000	0.00000	-	-	-
Percentage reduction (%)		-	9%	31%	44%	53%	62%	69%	71%	74%	79%	81%	82%	75%	74%	72%

Table 7. Table of results for District level hospital.

| Case		1	2	3	4	5	6	7	8	9	10	11	12	13	Optimal	14
ZONE A (1232 kW)	Optimal PV-DG in kWp (Bus)	-	185 (bus 2)	246 (bus 2)	308 (bus 2)	370 (bus 2)	431 (bus 2)	493 (bus 2)	554 (bus 2)	616 (bus 2)	678 (bus 5)	739 (bus 5)	801 (bus 5)	862 (bus 5)	885 (bus 5)	924 (bus 5)
Total Power Losses (kW)	ABC	648	645	642	511	401	313	243	193	164	138	99	73	62	60	121
	PSO	648	-	-	-	-	-	-	-	-	-	-	-	-	60	-
Voltage (P.U)	V min		0.9995	0.9998	0.9995	0.9992	0.9995	0.9995	0.9995	0.9995	0.9995	0.9995	0.9995	0.9995	0.9995	-
	V max		1	1	1	1	1	1	1	1	1	1	1	1	1	-
∑ kW Losses			0.00000	0.00000	0.00000	0.00000	0.00000	0.00000	0.00000	0.00000	0.00000	0.00000	0.00000	0.00000	0.00000	-
Percentage reduction (%)		-	0.5%	1%	21%	38%	52%	63%	70%	75%	79%	85%	89%	90%	91%	81%

8.4. Discussion on Simulated U-Trajectory Losses Curve Result

Since the simulated optimal outcome value for P_{DG2} in National, State, and District level hospitals was different in case position, some of the case by case numbers needed to shift forward to fit in the optimal value and for the ease in graphical plotting of U-Trajectory losses curve towards achieving clear understanding. Thus, the example of a new arrangement for case by case number for National level hospital is as in Table 8. Similarly, the State and District level hospitals use the same method for the new case by case number arrangement.

Table 8. Example of shifted case by case study to locate the simulated optimal value in the sequence.

National Level Hospital (Zone A)														
Original Case by Case Setup														
1	2	3	4	5	6	7	8	9	10	11	12	13	14	
New forward shifted arrangement (Optimal Value at Case 9)														
1	2	3	4	5	6	7	8	9	10	11	12	13	14	15

National Level Hospital (Zone B) Original Case by Case Setup														
1	2	3	4	5	6	7	8	9	10	11	12	13	14	
New forward shifted arrangement (Optimal Value at Case 10)														
1	2	3	4	5	6	7	8	9	10	11	12	13	14	15

From the previous analysis, the values of total line losses, L_3 versus simulation cases (PV-DG capacity and location) for all level hospitals are graphically plotted as in Figures 10–12 where the results confirmed the energy losses variation as a function of the PV-DG penetration level forms a U-shape trajectory in all the situations in accordance to other published work [3,17,21,22]. Other supporting literature was also obtained from [18] where power flow in a traditional distribution network was unidirectional and determined by the load profile due to centralized and passive with radial topology in the traditional development of the distribution networks.
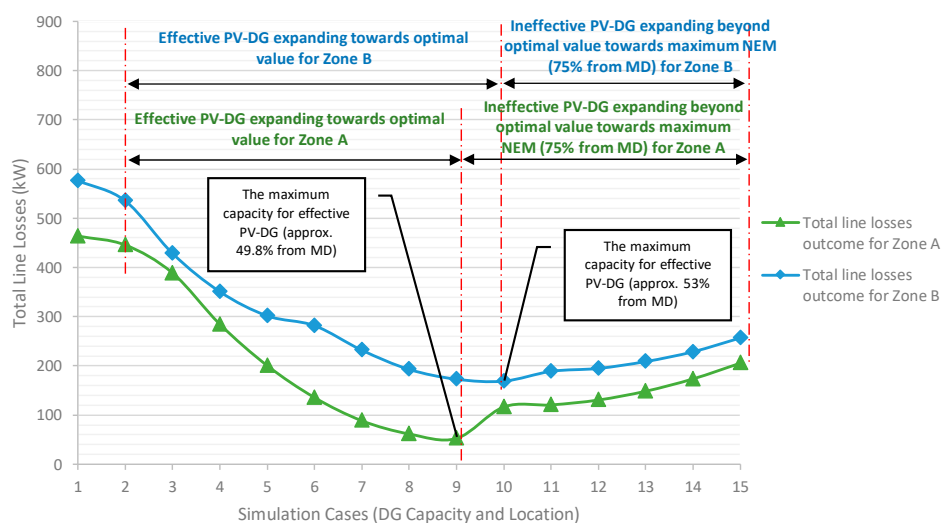
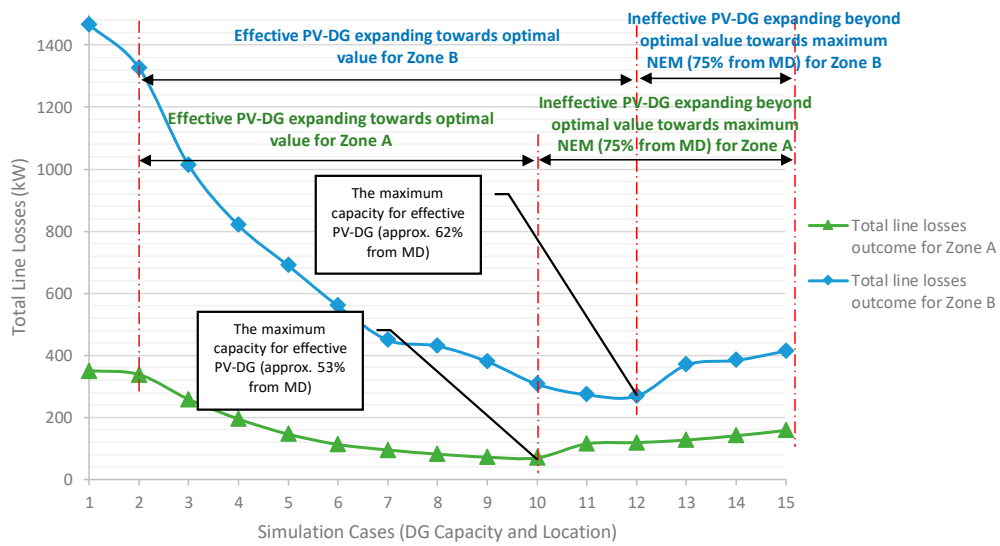**Figure 10.** Interpretation of losses curve outcome for National level hospital.

Figure 11. Interpretation of losses curve outcome for State level hospital.
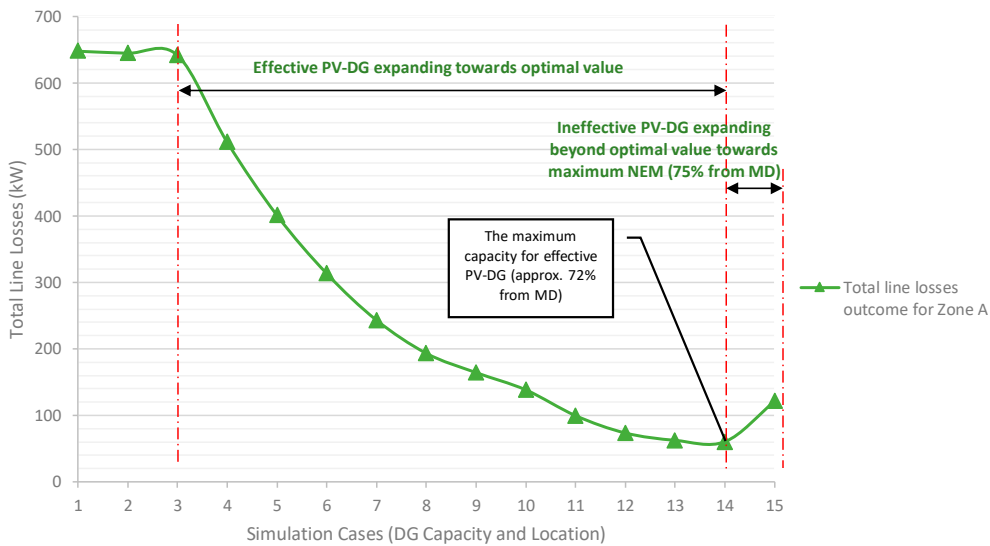

Figure 12. Interpretation of losses curve outcome for District level hospital.

With the presence of PV-DG, the power system is changing, i.e., a large number of PV-DG units are commonly connected to a distribution network which transform into an active modern distribution network with bidirectional power flows defined by the load profile and power generation of the DG units [19].

Variation of assigned cases represented by the NEM scheme in ascending order requirement reduced the total line losses and in the range of lower losses region curve which lay between the base case and the optimal loss value. However, the extensiveness of the NEM scheme as the focus subject and guided by the graphical U-trajectory losses curve (Figures 10–12) confirmed that the current NEM scheme for maximum PV-DG capacity (i.e., 75% from MD) is not effectively compatible towards optimal total line losses in the radial distribution network from selected public hospitals. This was also determined by the position (simulation cases) of the optimal PV-DG in each figure (Figures 10–12) and defined the expansion-limit for PV-DG integration for these selected distribution networks. Subject to total line losses reduction as main objective function, the position for PV-DG optimal value as well as the expansion-limit is different in every level and Zoning, due to the type and extensiveness of the radial distributed network in terms of R/X value as referred to by Box [96], also the *P* and *Q* load data in accordance with Thong et al. [21] and Bawan [41]. This optimal value is also dependent on

the overall performance of PV-DG integration in forming a bidirectional of *P* into these distribution networks as has been highlighted in [45].

According to the simulated graphical result for National level hospital (Figure 10), the property of Zone A distribution network in terms of bus and line data as previously mentioned, result in limiting the effective PV-DG expanding up to Case 9 (approximately 49.8% from MD) which lay between Case 8 (45% from MD) and Case 10 (50% from MD). While in Zone B, PV-DG can only be expanded up to Case 10 (optimal) with approximately 53% from MD. This has shown that the maximum PV-DG capacity as required under the NEM scheme is technically ineffective for National hospital distribution networks, since only the maximum of approximately 49.8% and 53% from MD is effective for Zone A and Zone B, respectively.

Whereas in State level hospital (Figure 11), the optimal values as well as the limit for expanded PV-DG capacity for both Zone A and Zone B, are Case 10 (i.e., 52% from MD) and Case 12 (i.e., 62% from MD) respectively. Thus, this has shown that the maximum PV-DG capacity as required under the NEM scheme is also technically ineffective for State hospital distribution networks, since only the maximum of approximately 52% and 62% from MD as well as the optimal value is a limit for Zone A and Zone B, respectively.

Lastly, for District level hospital (Figure 12), the optimal values, as well as the limit for expanded PV-DG capacity for Zone A, is Case 14 (i.e., 72% from MD). Thus, District hospital distribution networks could integrate PV-DG with almost the fully maximum requirement via the NEM scheme. In summary the proposed expansion-limit for all selected distribution networks were tailored by their own parameters and load profiles, and the limitation in adopting the NEM scheme for PV-DG capacity for each selected Zone can be well explained by comparison between maximum requirement of the NEM scheme and the actual PV-DG expansion-limit for effective outcome, as shown in Table 9.

Table 9. Comparison of NEM maximum PV-DG capacity and actual PV-DG expansion-limit for an effective outcome.

Hospital Level	NEM Scheme (Max. Capacity)	Expansion-Limit (Effective Capacity)
National Hospital Level	75% from MD (823 kWp)	**Zone A** 49.8% from MD (546 kWp)
	75% from MD (1193 kWp)	**Zone B** 53% from MD (840 kWp)
State Hospital Level	75% from MD (936 kWp)	**Zone A** 53% from MD (654 kWp)
	75% from MD (1938 kWp)	**Zone B** 62% from MD (1600 kWp)
District Hospital Level	75% from MD (924 kWp)	**Zone A** 72% from MD (885 kWp)

9. Conclusions

The reduction of total line losses, L_3 upon the integration of PV-DG towards the optimal value confirmed the significant loss improvement impact which is in line with the recent literature [21,50,97]. However, the gap in confirming the effectiveness and the efficient use of the current NEM scheme in full capacity was the focus for the desired outcome to be achieved in this paper. It can be seen that different characteristics of the radial distribution network in terms of size, line, and bus data contributed to the variation of the optimal case position whether to appear closer or further with the maximum capacity of 75% from MD (Case 15). For instance, the more complex the radial distribution network such as National level hospital (Zone A), the further the simulated optimal value (i.e., Case 9) was positioned from the said current 75% capacity requirement. Oppositely, the smaller network such as State level hospital was seen to be capable of achieving the optimal value position closer to the maximum value i.e., Case 10 and Case 12 for Zone A and Zone B, respectively. Lastly, the least

complex network i.e., District level hospital showed that the optimal value is the closest (i.e., Case 14) to the maximum NEM capacity (i.e., Case 15). In other words, these obtained results portrayed that the maximal application of the NEM scheme is more likely compatible with smaller and less complex radial distribution networks as compared to more complex and bigger radial distributed networks. As such, NEM is ineffective to be fully adopted into selected Malaysian public hospitals.

Oppositely, for other types of buildings such as houses, offices, and smaller commercial buildings, the utilization of the NEM requirement for maximum PV-DG capacity as currently imposed has never been published with any ineffective feedback by PV-DG penetration. This can be theoretically explained using the optimal outcome position of the District level hospital where the less complex distribution network significantly closes the gap between optimal and actual expansion-limit position, and even potentially provides a more expandable buffer in utilizing PV-DG even beyond the required maximum capacity (i.e., >75% of MD). Other than the complexity issue, the load type and the exponent value of *P* and *Q* as stipulated in Table 2, which was applied in Equations (2) and (3), determine the discrepancies in optimal outcome condition between the public hospital's distributed network case with others.

Thus, this portrayed the uniqueness of the solution towards an effective PV-DG outcome for selected public hospitals as compared to other types of buildings. Hence, optimization for location and output simultaneously partially solved the way forward for PV-DG expansion capacity via a NEM scheme in selected public hospitals to a certain limit of effectiveness. This limit shall give beneficial information to the RE developer in providing the best option for expanding PV-DG installation via a NEM scheme as well as providing the lowest power loss impact in the existing network. This can be seen by choosing the options criteria (list of cases) towards the optimal value, and this approach is practically proven for application.

Appendix A

Table A1. Bus and line data for National hospital level.

Zone	Zone A				Zone B			
Input Data	**Bus 4**	**Bus 5**	**Bus 6**	**Bus 7**	**Bus 11**	**Bus 12**	**Bus 13**	**Bus 14**
Voltage (kV)	11.2	11.2	11.2	11.2	11.2	11.3	11.2	11.2
P Load (kW)	100	472	105	420	499	465	539	87
Q Load (kVAR)	52	170	−46	240	−68	157	111	52
Resistance, *R* (Ω/km)	Bus 4–5 = 0.049, Bus 5–6 = 0.098, Bus 6–7 = 0.0686				Bus 11–12 = 0.049, Bus 12–13 = 0.0686, Bus 13–14 = 0.049			
Reactance, *X* (Ω/km)	Bus 4–5 = 0.0377, Bus 5–6 = 0.0754, Bus 6–7 = 0.0528				Bus 11–12 = 0.0377, Bus 12–13 =0.0528, Bus 13–14 = 0.0377			

Table A2. Bus and line data for State hospital level.

Zone	Zone A				Zone B				
Input Data	**Bus 1**	**Bus 2**	**Bus 3**	**Bus 4**	**Bus 5**	**Bus 6**	**Bus 7**	**Bus 8**	**Bus 9**
Voltage (kV)	10.9	10.9	10.9	10.9	10.9	10.9	10.9	10.9	10.9
P Load (kW)	710	187	151.5	199	1190	465	457	283	189
Q Load (kVAR)	22.5	98	77	125	20.9	130	175	137	63
Resistance, *R* (Ω/km)	Bus 1–2 = 0.049, Bus 2–3 = 0.0196, Bus 3–4 = 0.0294				Bus 5–6 = 0.0294, Bus 6–7 = 0.0196, Bus 7–8 = 0.049, Bus 8–9 = 0.0294				
Reactance, *X* (Ω/km)	Bus 1–2 = 0.0377, Bus 2–3 = 0.0151, Bus 3–4 = 0.0226				Bus 11–12 = 0.0377, Bus 12–13 = 0.0528, Bus 13–14 = 0.0377				

Table A3. Bus and line data for District hospital level.

Zone	Zone A			
Input Data	**Bus 2**	**Bus 3**	**Bus 4**	**Bus 5**
Voltage (kV)	10.9	10.9	10.9	10.9
P Load (kW)	217	50	479	485
Q Load (kVAR)	33.42	10	181	198
Resistance, *R* (Ω/km)	Bus 3–4 = 0.0196, Bus 4–5 = 0.0686, Bus 5–2 = 0.049			
Reactance, *X* (Ω/km)	Bus 3–4 = 0.0151, Bus 4–5 = 0.0528, Bus 5–2 = 0.0377			

References

1. Manaf, N.H.A. Quality management in Malaysian public health care. *Int. J. Health Care Qual. Assur. Inc. Leadsher. Health Serv.* **2005**, *18*, 204–216. [CrossRef]
2. Aripin, S. Healing architecture: A study on the physical aspects of healing environment in hospital design. In Proceedings of the 40th Annual Conference of the Architectural Science Association (ANZAScA), Adelaide, South Australia, 22–25 November 2006; Australia Shannon, S., Soebarto, V., Williamson, T., Eds.; Architectural Science Association (ASA): Adelaide, Australia, 2006; pp. 342–349.
3. Amran, M.E.; Muhtazaruddin, M.N. Assessment of renewable distributed generation in green building rating system for public hospital. *Int. J. Eng. Technol.* **2018**, *7*, 40–45. [CrossRef]
4. Wu, Z. *Evaluation of A Sustainable Hospital Design Based on its Social and Environmental Outcomes*; Cornell University: Ithaca, NY, USA, 2011.
5. Tenaga Nasional Berhad (TNB). *Electricity Supply Application Handbook*, 3rd ed.; Nur-Johan Sdn Bhd: Kuala Lumpur, Malaysia, 2011.
6. Energy Commission. *Electricity Supply Act 1990—Efficient Management of Electrical Energy Regulation 2008*; Government of Malaysia: Kuala Lumpur, Malaysia, 2008; pp. 1–28.
7. Sahamir, S.R.; Zakaria, R. Green Assessment Criteria for Public Hospital Building Development in Malaysia. *Procedia Environ. Sci.* **2014**, *20*, 106–115. [CrossRef]
8. Economic Planning Unit (EPU). *Eleventh Malaysia Plan 2016–2020: Anchoring Growth on People*; Prime Minister's Department: Putrajaya, Malaysia, 2015.
9. Petinrin, J.O.; Shaaban, M. Renewable energy for continuous energy sustainability in Malaysia. *Renew. Sustain. Energy Rev.* **2015**, *50*, 967–981. [CrossRef]
10. Hashim, H.; Ho, W.S. Renewable energy policies and initiatives for a sustainable energy future in Malaysia. *Renew. Sustain. Energy Rev.* **2011**, *15*, 4780–4787. [CrossRef]
11. Muhammad-Sukki, F.; Abu-Bakar, S.H.; Munir, A.B.; Mohd Yasin, S.H.; Ramirez-Iniguez, R.; McMeekin, S.G.; Stewart, B.G.; Abdul Rahim, R. Progress of feed-in tariff in Malaysia: A year after. *Energy Policy* **2014**, *67*, 618–625. [CrossRef]
12. Ministry of Energy, Science, Technology, Environment & Climate Change (MESTECC). *Initiatif MESTECC 2019*; MESTECC: Kuala Lumpur, Malaysia, 2019.
13. Sustainable Energy Development Authority (SEDA) Malaysia. National Renewable Energy Policy. Available online: http://www.seda.gov.my/policies/national-renewable-energy-policy-and-action-plan-2009/ (accessed on 3 June 2019).
14. Shi, L.; Chew, M.Y.L. A review on sustainable design of renewable energy systems. *Renew. Sustain. Energy Rev.* **2012**, *16*, 192–207. [CrossRef]

15. GhaffarianHoseini, A.; Dahlan, N.D.; Berardi, U.; GhaffarianHoseini, A.; Makaremi, N.; GhaffarianHoseini, M. Sustainable energy performances of green buildings: A review of current theories, implementations and challenges. *Renew. Sustain. Energy Rev.* **2013**, *25*, 1–17. [CrossRef]

16. Muhtazaruddin, M.N.B.; Tuyen, N.D.; Fujita, G.; Jamian, J.J. Bin Optimal Distributed Generation and capacitor coordination for power loss minimization. In Proceedings of the 2014 IEEE PES T&D Conference and Exposition, Chicago, IL, USA, 14–17 April 2014; pp. 1–5.

17. Quezada, V.H.M.; Abbad, J.R.; Roman, T.G.S. Assessment of energy distribution losses for increasing penetration of distributed generation. *IEEE Trans. Power Syst.* **2006**, *21*, 533–540.

18. Ho, W.S.; Hashim, H.; Hassim, M.H.; Muis, Z.A.; Shamsuddin, N.L.M. Design of distributed energy system through Electric System Cascade Analysis (ESCA). *Appl. Energy* **2012**, *99*, 309–315. [CrossRef]

19. Savić, A.; Đurišić, Ž. Optimal sizing and location of SVC devices for improvement of voltage profile in distribution network with dispersed photovoltaic and wind power plants. *Appl. Energy* **2014**, *134*, 114–124. [CrossRef]

20. Hossain, M.J.; Saha, T.K.; Mithulananthan, N.; Pota, H.R. Robust control strategy for PV system integration in distribution systems. *Appl. Energy* **2012**, *99*, 355–362. [CrossRef]

21. Van Thong, V.; Driesen, J.; Belmans, R. Interconnection of distributed generators and their influences on power system. *Int. Energy J.* **2005**, *6*, 3127–3138.

22. Mahdad, B.; Srairi, K. Adaptive differential search algorithm for optimal location of distributed generation in the presence of SVC for power loss reduction in distribution system. *Eng. Sci. Technol. Int. J.* **2016**, *19*, 1266–1282. [CrossRef]

23. Wu, Y.-K.; Lin, J.-H.; Lin, H.-J. Standards and guidelines for grid-connected photovoltaic generation systems: A review and comparison. *IEEE Trans. Ind. Appl.* **2017**, *53*, 3205–3216. [CrossRef]

24. Zaini, N.H.; Ab. Kadir, M.Z.A.; Mohd Radzi, M.A.; Izadi, M.; Azis, N.; Ahmad, N.I.; Mohd Nasir, M.S. Lightning surge analysis on a large scale grid-connected solar photovoltaic system. *Energies* **2017**, *10*, 2149. [CrossRef]

25. Tan, R.H.G.; Chow, T.L. A Comparative Study of Feed in Tariff and Net Metering for UCSI University North Wing Campus with 100 kW Solar Photovoltaic System. *Energy Procedia* **2016**, *100*, 86–91. [CrossRef]

26. Oh, T.H.; Hasanuzzaman, M.; Selvaraj, J.; Teo, S.C.; Chua, S.C. Energy policy and alternative energy in Malaysia: Issues and challenges for sustainable growth—An update. *Renew. Sustain. Energy Rev.* **2018**, *81*, 3021–3031. [CrossRef]

27. Christoforidis, G.C.; Chrysochos, A.; Papagiannis, G.; Hatzipanayi, M.; Georghiou, G.E. Promoting PV energy through net metering optimization: The PV-NET project. In Proceedings of the IEEE 2013 International Conference on Renewable Energy Research and Applications (ICRERA), Madrid, Spain, 20–23 October 2013; pp. 1117–1122.

28. Poullikkas, A.; Kourtis, G.; Hadjipaschalis, I. A review of net metering mechanism for electricity renewable energy sources. *Int. J. Energy Environ.* **2013**, *4*, 975–1002.

29. Prasad, M.; Munch, S. State-level renewable electricity policies and reductions in carbon emissions. *Energy Policy* **2012**, *45*, 237–242. [CrossRef]

30. Van der Veen, R.A.C.; De Vries, L.J. The impact of microgeneration upon the Dutch balancing market. *Energy Policy* **2009**, *37*, 2788–2797. [CrossRef]

31. Poullikkas, A.; Kourtis, G.; Hadjipaschalis, I. An overview of the EU Member States support schemes for the promotion of renewable energy sources. *Int. J. Energy Environ.* **2012**, *3*, 553–566.

32. Huijben, J.C.C.M.; Verbong, G.P.J. Breakthrough without subsidies? PV business model experiments in the Netherlands. *Energy Policy* **2013**, *56*, 362–370. [CrossRef]

33. Elkinton, M.R.; McGowan, J.G.; Manwell, J.F. Wind power systems for zero net energy housing in the United States. *Renew. Energy* **2009**, *34*, 1270–1278. [CrossRef]

34. Vachon, S.; Menz, F.C. The role of social, political, and economic interests in promoting state green electricity policies. *Environ. Sci. Policy* **2006**, *9*, 652–662. [CrossRef]

35. Zahedi, A. A review on feed-in tariff in Australia, what it is now and what it should be. *Renew. Sustain. Energy Rev.* **2010**, *14*, 3252–3255. [CrossRef]

36. Zhao, J.; Mazhari, E.; Celik, N.; Son, Y.-J. Hybrid agent-based simulation for policy evaluation of solar power generation systems. *Simul. Model. Pract. Theory* **2011**, *19*, 2189–2205. [CrossRef]

37. Prindle, W.; Koszalka, M. Succeeding in the Smart Grid Space by Listening to Customers and Stakeholders. In *Smart Grid: Integrating Renewable, Distributed & Efficient Energy*; Sioshansi, F.P., Ed.; Academic Press: Oxford, UK, 2012; pp. 343–369.

38. Greacen, C.; Plevin, R.; Greacen, C.S. Thai power: Net metering comes to Thailand. *Refocus* **2003**, *4*, 34–37. [CrossRef]

39. EC Electricity Supply Act 1990 [Act 447]. *Guidelines for Solar Photovoltaic Installation on Net Energy Metering Scheme*; GP/ST/ No. 4/2016 (Pin. 2019); Government of Malaysia: Putrajaya, Malaysia, 2019; pp. 1–231.

40. Tenaga Nasional Berhad (TNB). *Technical Guideline for Connection of Indirect Solar PV Power Generation for Net Energy Metering Chapter*; TNB: Kuala Lumpur, Malaysia, 2019.

41. Bawan, E.K. Distributed Generation Impact on Power System Case Study: Losses and Voltage Profile. In Proceedings of the IEEE 2012 22nd Australasian Universities Power Engineering Conference (AUPEC), Bali, Indonesia, 26–29 September 2012; pp. 1–6.

42. Griffin, T.; Tomsovic, K.; Secrest, D.; Law, A. Placement of dispersed generation systems for reduced losses. In Proceedings of the 33rd Annual Hawaii International Conference on System Sciences, IEEE Computer Society, Maui, HI, USA, 7 January 2000; Volume 1, p. 9.

43. Hung, D.Q.; Mithulananthan, N. Multiple distributed generator placement in primary distribution networks for loss reduction. *IEEE Trans. Ind. Electron.* **2013**, *60*, 1700–1708. [CrossRef]

44. Parizad, A.; Khazali, A.; Kalantar, M. Optimal placement of distributed generation with sensitivity factors considering voltage stability and losses indices. In Proceedings of the IEEE 2010 18th Iranian Conference on Electrical Engineering, Isfahan, Iran, 11–13 May 2010; pp. 848–855.

45. Acharya, N.; Mahat, P.; Mithulananthan, N. An analytical approach for DG allocation in primary distribution network. *Int. J. Electr. Power Energy Syst.* **2006**, *28*, 669–678. [CrossRef]

46. Ramesh, L.; Chowdhury, S.P.; Chowdhury, S.; Natarajan, A.A.; Gaunt, C.T. Minimization of power loss in distribution networks by different techniques. *Int. J. Electr. Comput. Eng.* **2009**, *3*, 661–667.

47. González-Longatt, F.M. Impact of Distributed Generation over Power Losses on Distribution System. In Proceedings of the 9th International Conference on Electrical Power Quality and Utilization, Barcelona, Spain, 2007; pp. 1–6.

48. Singh, D.; Singh, D.; Verma, K.S. Multiobjective optimization for DG planning with load models. *IEEE Trans. Power Syst.* **2009**, *24*, 427–436. [CrossRef]

49. Abdi, S.; Afshar, K. Application of IPSO-Monte Carlo for optimal distributed generation allocation and sizing. *Int. J. Electr. Power Energy Syst.* **2013**, *44*, 786–797. [CrossRef]

50. Rama Prabha, D.; Jayabarathi, T. Optimal placement and sizing of multiple distributed generating units in distribution networks by invasive weed optimization algorithm. *Ain Shams Eng. J.* **2016**, *7*, 683–694. [CrossRef]

51. Krueasuk, W.; Ongsakul, W. Optimal Placement of Distributed Generation Using Particle Swarm Optimization. In Proceedings of the Australasian Universities Power Engineering Conference (AUPEC 2006, Melbourne, Australia, 10–13 December 2006; pp. 1–6.

52. Sa'ed, J.A.; Jubran, M.K.; Favuzza, S.; Massaro, F. Reassessment of Voltage Stability for Distribution Networks in Presence of DG. In Proceedings of the 2016 IEEE 16th International Conference on Environment and Electrical Engineering (EEEIC), Florence, Italy, 7–10 June 2016; pp. 1–5.

53. Hien, N.C.; Mithulananthan, N.; Bansal, R.C. Location and sizing of distributed generation units for loadabilty enhancement in primary feeder. *IEEE Syst. J.* **2013**, *7*, 797–806. [CrossRef]

54. Syahputra, R.; Robandi, I.; Ashari, M. Performance improvement of radial distribution network with distributed generation integration using extended particle swarm optimization algorithm. *Int. Rev. Electr. Eng.* **2015**, *10*, 293–304. [CrossRef]

55. Wu, Y.-K.; Ye, G.-T.; Shaaban, M. Analysis of impact of integration of large PV generation capacity and optimization of PV capacity: Case studies in Taiwan. *IEEE Trans. Ind. Appl.* **2016**, *52*, 4535–4548. [CrossRef]

56. Katiraei, F.; Aguero, J. Solar PV integration challenges. *IEEE Power Energy Mag.* **2011**, *9*, 62–71. [CrossRef]

57. Demirok, E.; Sera, D.; Teodorescu, R.; Rodriguez, P.; Borup, U. Clustered PV inverters in LV networks: An overview of impacts and comparison of voltage control strategies. In Proceedings of the 2009 IEEE Electrical Power & Energy Conference (EPEC), Montreal, QC, Canada, 22–23 October 2009; pp. 1–6.

58. Liew, S.N.; Strbac, G. Maximising penetration of wind generation in existing distribution networks. *IEE Proc.-Gener. Transm. Distrib.* **2002**, *149*, 256. [CrossRef]

59. Bonfiglio, A.; Brignone, M.; Delfino, F.; Procopio, R. Optimal control and operation of grid-connected photovoltaic production units for voltage support in medium-voltage networks. *IEEE Trans. Sustain. Energy* **2014**, *5*, 254–263. [CrossRef]

60. Agalgaonkar, Y.P.; Pal, B.C.; Jabr, R.A. Distribution voltage control considering the impact of PV generation on tap changers and autonomous regulators. *IEEE Trans. Power Syst.* **2014**, *29*, 182–192. [CrossRef]

61. Farivar, M.; Neal, R.; Clarke, C.; Low, S. Optimal Inverter VAR Control in Distribution Systems with High PV Penetration. In Proceedings of the 2012 IEEE Power and Energy Society General Meeting, San Diego, CA, USA, 22–26 July 2012; pp. 1–7.

62. Yeh, H.-G.; Gayme, D.F.; Low, S.H. Adaptive VAR control for distribution circuits with photovoltaic generators. *IEEE Trans. Power Syst.* **2012**, *27*, 1656–1663. [CrossRef]

63. Nguyen, T.T.; Truong, A.V.; Phung, T.A. A novel method based on adaptive cuckoo search for optimal network reconfiguration and distributed generation allocation in distribution network. *Int. J. Electr. Power Energy Syst.* **2016**, *78*, 801–815. [CrossRef]

64. Rao, R.S.; Ravindra, K.; Satish, K.; Narasimham, S.V.L. Power loss minimization in distribution system using network reconfiguration in the presence of distributed generation. *IEEE Trans. Power Syst.* **2013**, *28*, 317–325. [CrossRef]

65. Sultana, U.; Khairuddin, A.B.; Aman, M.M.; Mokhtar, A.S.; Zareen, N. A review of optimum DG placement based on minimization of power losses and voltage stability enhancement of distribution system. *Renew. Sustain. Energy Rev.* **2016**, *63*, 363–378. [CrossRef]

66. Usman, M.; Coppo, M.; Bignucolo, F.; Turri, R. Losses management strategies in active distribution networks: A review. *Electr. Power Syst. Res.* **2018**, *163*, 116–132. [CrossRef]

67. Moghimi, S.; Mat, S.; Lim, C.H.; Zaharim, A.; Sopian, K. Building Energy Index (BEI) in Large Scale Hospital: Case Study of Malaysia. In Proceedings of the 4th WSEAS International Conference on Engineering Mechanics, Structures, Engineering Geology (EMESEG'11) and 2nd International Conference on Geography and Geology 2011, Corfu Island, Greece, 14–17 July 2011; pp. 167–170.

68. Iqbal, F.; Khan, M.T.; Siddiqui, A.S. Optimal placement of DG and DSTATCOM for loss reduction and voltage profile improvement. *Alex. Eng. J.* **2018**, *57*, 755–765. [CrossRef]

69. Popovich, B.; Hjemvick, J.A.; Faylo, S.E.; Lathrop, T.M. Transfer switch controller employing active inductive load control and transfer switch including the same. U.S. Patent No. 7,948,117, 24 May 2011.

70. Moradi, M.H.; Abedini, M. A combination of genetic algorithm and particle swarm optimization for optimal DG location and sizing in distribution systems. *Int. J. Electr. Power Energy Syst.* **2012**, *34*, 66–74. [CrossRef]

71. Dixit, M.; Kundu, P.; Jariwala, H.R. Optimal Placement of PV array in Distribution System for Power Loss Minimization Considering Feeder Reconfiguration. In Proceedings of the 2016 IEEE 16th International Conference on Environment and Electrical Engineering (EEEIC), Florence, Italy, 7–10 June 2016; pp. 1–6.

72. Baños, R.; Manzano-Agugliaro, F.; Montoya, F.G.; Gil, C.; Alcayde, A.; Gómez, J. Optimization methods applied to renewable and sustainable energy: A review. *Renew. Sustain. Energy Rev.* **2011**, *15*, 1753–1766. [CrossRef]

73. Bhowmik, C.; Bhowmik, S.; Ray, A.; Pandey, K.M. Optimal green energy planning for sustainable development: A review. *Renew. Sustain. Energy Rev.* **2017**, *71*, 796–813. [CrossRef]

74. Yasin, Z.M.; Rahman, T.K.A.; Musirin, I.; Rahim, S.R.A. Optimal Sizing of Distributed Generation by Using Quantum-Inspired Evolutionary Programming. In Proceedings of the 2010 4th International Power Engineering and Optimization Conference (PEOCO), Shah Alam, Malaysia, 23–24 June 2010; pp. 468–473.

75. Muhtazaruddin, M.N.B.; Jamian, J.J.B.; Fujita, G. Determination of optimal output power and location for multiple distributed generation sources simultaneously by using artificial bee colony. *IEEJ Trans. Electr. Electron. Eng.* **2014**, *9*, 351–359. [CrossRef]

76. Muttaqi, K.M.; Le, A.D.T.; Aghaei, J.; Mahboubi-Moghaddam, E.; Negnevitsky, M.; Ledwich, G. Optimizing distributed generation parameters through economic feasibility assessment. *Appl. Energy* **2016**, *165*, 893–903. [CrossRef]

77. Kansal, S.; Sai, B.B.R.; Tyagi, B.; Kumar, V. Optimal placement of distributed generation in distribution networks. *Int. J. Eng. Sci. Technol.* **2011**, *3*, 47–55. [CrossRef]

78. Zareiegovar, G.; Fesaghandis, R.R.; Azad, M.J. Optimal DG Location and Sizing in Distribution System to Minimize Losses, Improve Voltage Stability, and Voltage Profile. In Proceedings of the IEEE 17th Conference on Electrical Power Distribution, Tehran, Iran, 2–3 May 2012; pp. 1–6.

79. El-Zonkoly, A.M. Optimal placement of multi-distributed generation units including different load models using particle swarm optimisation. *IET Gener. Transm. Distrib.* **2011**, *5*, 760. [CrossRef]

80. Kansal, S.; Kumar, V.; Tyagi, B. Optimal placement of different type of DG sources in distribution networks. *Int. J. Electr. Power Energy Syst.* **2013**, *53*, 752–760. [CrossRef]

81. Merei, G.; Berger, C.; Sauer, D.U. Optimization of an off-grid hybrid PV–Wind–Diesel system with different battery technologies using genetic algorithm. *Sol. Energy* **2013**, *97*, 460–473. [CrossRef]

82. Yang, H.; Wei, Z.; Chengzhi, L. Optimal design and techno-economic analysis of a hybrid solar–wind power generation system. *Appl. Energy* **2009**, *86*, 163–169. [CrossRef]

83. Yang, H.; Zhou, W.; Lu, L.; Fang, Z. Optimal sizing method for stand-alone hybrid solar–wind system with LPSP technology by using genetic algorithm. *Sol. Energy* **2008**, *82*, 354–367. [CrossRef]

84. Koutroulis, E.; Kolokotsa, D.; Potirakis, A.; Kalaitzakis, K. Methodology for optimal sizing of stand-alone photovoltaic/wind-generator systems using genetic algorithms. *Sol. Energy* **2006**, *80*, 1072–1088. [CrossRef]

85. Koutroulis, E.; Kolokotsa, D. Design optimization of desalination systems power-supplied by PV and W/G energy sources. *Desalination* **2010**, *258*, 171–181. [CrossRef]

86. Ould Bilal, B.; Sambou, V.; Ndiaye, P.A.; Kébé, C.M.F.; Ndongo, M. Optimal design of a hybrid solar–wind-battery system using the minimization of the annualized cost system and the minimization of the loss of power supply probability (LPSP). *Renew. Energy* **2010**, *35*, 2388–2390. [CrossRef]

87. Biswas, S.; Goswami, S.K.; Chatterjee, A. Optimum distributed generation placement with voltage sag effect minimization. *Energy Convers. Manag.* **2012**, *53*, 163–174. [CrossRef]

88. Hussain, I.; Roy, A.K. Optimal Distributed Generation Allocation in Distribution Systems Employing Modified Artificial Bee Colony Algorithm to Reduce Losses and Improve Voltage Profile. In Proceedings of the IEEE-International Conferences on Advances in Engineering, Science and Management (ICAESM), 2012, Nagapattinam, Tamil Nadu, India, 30–31 March 2012; pp. 565–570.

89. Karaboga, D.; Basturk, B. Artificial Bee Colony (ABC) Optimization Algorithm for Solving Constrained Optimization Problems. In *Foundations of Fuzzy Logic and Soft Computing*; Melin, P., Castillo, O., Aguilar, L.T., Kacprzyk, J., Pedrycz, W., Eds.; Springer: Berlin/Heidelberg, Germany, 2007; pp. 789–798.

90. Lalitha, M.P.; Reddy, N.S.; Reddy, V.C.V. Optimal DG placement for maximum loss reduction in radial distribution system using ABC algorithm. *Int. J. Rev. Comput.* **2009**, *3*, 44–52.

91. Sohi, M.F.; Shirdel, M.; Javidaneh, A. Applying BCO Algorithm to Solve the Optimal DG Placement and Sizing Problem. In Proceedings of the IEEE 2011 5th International Power Engineering and Optimization Conference, Shah Alam, Selangor, Malaysia, 6–7 June 2011; pp. 71–76.

92. Abu-Mouti, F.S.; El-Hawary, M.E. Optimal distributed generation allocation and sizing in distribution systems via artificial bee colony algorithm. *IEEE Trans. Power Deliv.* **2011**, *26*, 2090–2101. [CrossRef]

93. Nabil Muhtazaruddin, M.; Jamian, J.J.; Nguyen, D.; Jalalludin, N.A.; Fujita, G. Optimal capacitor placement and sizing via artificial bee colony. *Int. J. Smart Grid Clean Energy* **2014**, *3*, 200–206. [CrossRef]

94. Muhtazaruddin, M.N.; Bani, N.A.; Mohd Aris, S.A.; Abd. Jalil, S.Z.; Mad Kaidi, H.; Abd Fatah, A.Y.; Jamian, J.J.; Muhammad-Sukki, F.; Abu-Bakar, S.H. Distribution power loss minimization via distributed generation, capacitor and network reconfiguration. *Indones. J. Electr. Eng. Comput. Sci.* **2017**, *5*, 488–495. [CrossRef]

95. Rama Prabha, D.; Jayabarathi, T.; Umamageswari, R.; Saranya, S. Optimal location and sizing of distributed generation unit using intelligent water drop algorithm. *Sustain. Energy Technol. Assess.* **2015**, *11*, 106–113. [CrossRef]

96. Box, H.C. *Set Lighting Technician's Handbook: Film Lighting Equipment, Practice, and Electrical Distribution*; Routledge: London, UK, 2013; ISBN 9780240810751.

97. Aman, M.M.; Jasmon, G.B.; Bakar, A.H.A.; Mokhlis, H. A new approach for optimum DG placement and sizing based on voltage stability maximization and minimization of power losses. *Energy Convers. Manag.* **2013**, *70*, 202–210. [CrossRef]